THE HANBURY-BROWN TWISS EFFECT IN HEAVY ION COLLISIONS

by

Julian Charles Shillcock

B.Sc(Hons), King's College London, 1982

THESIS SUBMITTED IN PARTIAL FULFILLMENT OF

THE REQUIREMENTS FOR THE DEGREE OF

MASTER OF SCIENCE

in the Department

of

Physics

SIMON FRASER UNIVERSITY

November, 1984

APPROVAL

Name: Julian Charles Shillcock

Degree: Master of Science

Title of thesis: The Hanbury-Brown Twiss Effect in Heavy Ion Collisions

Examining Committee:

Chairperson: Bruce P. Clayman

David H. Boal
Senior Supervisor

Richard Woloshyn

Ralph G. Korteling

Byron Jennings
External Examiner
TRIUMF

Date Approved: November 2, 1984

PARTIAL COPYRIGHT LICENSE

I hereby grant to Simon Fraser University the right to lend my thesis, project or extended essay (the title of which is shown below) to users of the Simon Fraser University Library, and to make partial or single copies only for such users or in response to a request from the library of any other university, or other educational institution, on its own behalf or for one of its users. I further agree that permission for multiple copying of this work for scholarly purposes may be granted by me or the Dean of Graduate Studies. It is understood that copying or publication of this work for financial gain shall not be allowed without my written permission.

Title of Thesis/Project/Extended Essay

The Hanbury-Brown Twiss Effect in Heavy-Ion Collisions

Author: _____
(signature)

Julian Charles Shillcock
(name)

3/12/84
(date)

ABSTRACT

In this thesis we describe one method of extracting more detailed information from heavy ion collisions than is possible from single particle inclusive data. This method, the so-called Hanbury-Brown Twiss Effect, involves the measurement of correlations between identical particles emitted in the reaction with nearly equal momenta. We apply it to protons, deuterons and tritons emitted from high-energy heavy ion collisions and obtain information on the emitting region via the probability of observing two identical particles close together in phase space. This correlation is quite sensitive to the space-time structure of the emitting region. It may also be used to look for indications of thermalisation inside the reaction volume. The effect is shown to be strongly dependent on the identity of the emitted particles, it being much weaker for deuterons and tritons than protons. It appears that the heavier mass particles are emitted from a larger region than the lighter protons. This picture is consistent with the formation of a small, hot region - the "fireball", which emits particles while gradually expanding and cooling. A comparison with the available data from pp, dd and tt coincidence experiments is made and the source sizes and lifetimes are extracted.

DEDICATION

The heavens declare the glory of God
and the firmament proclaims his handiwork.

Ps 19:1

ACKNOWLEDGEMENTS

I would like to thank my supervisor David Boal first of all for giving me the problem to work on, and secondly for helping me with the more complicated parts. Also I want to thank the lecturers and students in the physics department for their encouragement and answers to many of my questions. Finally I must express my gratitude to the mathematics and physics departments of Simon Fraser University for the financial support I have received as a teaching assistant and research assistant during my two years in Canada.

Table Of Contents

List of Tables

List of Figures

1. Introduction

1.1 General

Experiments with heavy ions, defined in this thesis to be any nucleus heavier than helium, began in the 1960's with the pioneering scattering experiments of Bromley, Kuehner and Almqvist[1] using ^{12}C and ^{16}O at the Chalk River Nuclear Laboratory. They measured the excitation functions and angular distributions for protons, deuterons and gamma-rays from the reactions $^{12}C + ^{12}C$, $^{12}C + ^{16}O$, and $^{16}O + ^{16}O$. Most of the results of this and later experiments were explained semi-quantitatively using the optical model. This model compares the scattering of nuclei by nuclei to the diffraction of light by a partially absorbing disc.

Since then various semi-classical models have been proposed, some of which contain mutually exclusive assumptions. For example, the direct model pictures a nucleus-nucleus collision as a superposition of free nucleon-nucleon collisions and requires that each nucleon undergo at most one significant collision. Consequently, the nucleon mean free path is much larger than the linear dimension of the system. At the other extreme the thermal model needs a short mean free path so that the energy of a nucleon is lost gradually through many

collisions. Obviously it would be helpful to be able to distinguish between these processes, and to find out when a particular mechanism predominates. To do this it is not sufficient just to measure the energy spectra, multiplicity and angular distribution of the reaction products, because there are still very many ways the system may evolve into a state described by such coarse observables. With beam energies of 10 MeV per nucleon and fifty or more nucleons in each ion a description in terms of single particle inclusive data is very incomplete. We are reminded of the description of a gas by its pressure, volume and temperature which leaves the gas free to be in any one of a large number of microstates.

The next level of description of a heavy ion collision involves small-angle coincidence measurements. These are sensitive not only to the particles emitted, but also to any final state interactions of the particles, and more importantly, to the structure of the emitting region.

The dependence of two-particle coincidence rates on the source was first demonstrated in the 1950's by Hanbury-Brown and Twiss[2-3]. They measured the time of arrival of photons from a distant star in two detectors. The results showed that the times of arrival were correlated, there being more coincidences, and photon pairs, at small time seperations than was expected if the photons were emitted at randomly spaced times. With the advent of the laser it was found that this effect did not exist for the coherent light from a laser. It was attributed to the chaotic

nature of the source which shows large fluctuations in the intensity of the emitted light. At the peak of one of these fluctuations there is an enhanced probability of detecting a photon coincidence, hence the name photon bunching. For the constant intensity light from a laser there are no fluctuations and hence no photon bunching.

The possible application of this effect (called the HBT effect after its originators) to particles emitted in a heavy ion collision was pointed out by Cocconi[4] in the early seventies. He derived a simple example of an interference pattern in the coincidence spectra of identical pions emitted during a nuclear collision, and related the interference effect to the quantum mechanical path ambiguity which arises when detecting two identical particles from a chaotic source. From the interference effect he was able to calculate the angular diameter of the source.

Since then much work has been done on two-pion correlation measurements[5-8] and the search has been extended to protons[9,10] and just recently, to deuterons and tritons.[11] The results of these experiments show that small-angle two-particle coincidence measurements are quite sensitive to the space-time structure of the emitting region and may be used to determine the size and lifetime of this region. More tentatively it has been suggested[8] that the degree of coherence of the source, i.e. the departure from random emission of particles, might also be obtainable, and from this an indication of possible collective motion in the

nuclei such as hydrodynamic flow. Although the experimental results gained so far preclude strong assertions on collective motion, they do lead to fairly accurate estimates of the size of the emitting region.

Source sizes of the order of 3-5 fm have been found from proton[9-11] and pion[5-8] coincidence experiments. The question then arises whether larger fragments, such as deuterons and tritons, are emitted from roughly the same size region or a larger one. Because these particles are loosely bound (for deuterons the binding energy is 2.2 MeV) they tend to break up if emitted early on in the reaction when the temperature of the nucleus is high. Later on, when the temperature has dropped, emission of light, bound particles takes place. This would lead to larger source sizes for such particles than for protons or pions.

If this is found to be the case it supports the idea of a thermalised region of hot, dense nuclear matter created in the collision which emits particles while expanding and cooling down. The light particles would be emitted early on in the reaction from a small source, the heavier particles later from a larger source.

The lifetime of the source is also an important quantity to be determined as it may be used to discriminate between several currently popular models. In particular, if it is found to be short, say less than 90 fm/c, then the idea of the reaction proceeding by the formation of compound nuclei, which

subsequently decay emitting light fragments, may be discarded as this requires times of the order of 300 fm/c for each step. [12] Compound nucleus formation is the limit of extreme inelastic collisions. All the kinetic energy of the projectile is absorbed by the compound system which must have a lifetime long enough for complete internal equilibrium to take place. The break-up of this system is then independent of the entrance channel, except for conserved quantities like total mass, energy and charge.

Small-angle coincidence measurements are thus an important means of characterising heavy ion reaction mechanisms. However, it is possible that the effect is swamped by the interactions among the many particles emitted during such a collison. As was first pointed out by Koonin[13], final state interactions of the particles, rather than obscure the correlation effect, actually enhance it. Thus, although in photon measurements, and to a lesser extent in pion measurements, final state interactions may be neglected, or simply corrected for with a multiplicative normalising constant, in pp, dd and tt coincidence experiments these effects must be taken into account explicitly. When this is done, the results, although different from the simple HBT effect, are still capable of yielding quantitative information about the collision volume.

In the remainder of this introduction we describe the HBT effect for two identical, spinless particles, neglecting final state interactions. In Section 2 we describe the various semi-classical models of heavy ion reaction mechanisms and give

their strengths and weaknesses and discuss results from experiments which illustrate the various mechanisms involved. In Section 3 we derive the HBT effect for two protons taking into account the final state interactions and show how this leads to a modification of the simple picture presented in Section 1.2.

We calculate the effect assuming a Gaussian distribution function in space and time for the emission of a proton from the source volume. Then, because of the bad convergence properties of the solution for large values of the source lifetime, we derive the correlation function assuming a δ-function shape in space while keeping the Gaussian time dependence. In this latter case we lose any angular dependence of the emitting region but are enabled to calculate an upper limit for the source lifetime. We also extend the calculation to deuteron and triton coincidences with negligible source lifetimes, and compare the results for the different types of particles. Finally, in Section 4 we discuss our results and compare them to published data in pp, dd and tt coincidence experiments and extract the "Best Fit" source sizes and lifetimes. Appendix A contains the full calculations sketched in Section 3, and Appendix B contains examples of the computer programmes which were written for these calculations.

1.2 The Hanbury-Brown Twiss Effect

We outline here the calculation of the HBT effect for two identical spinless particles, for example, two photons from a star or two pions from a heavy ion collision. We include the case of two fermions but shall ignore spin for the moment. This is possible as we shall ignore final state interactions until later.

Consider the situation shown in Figure 1:

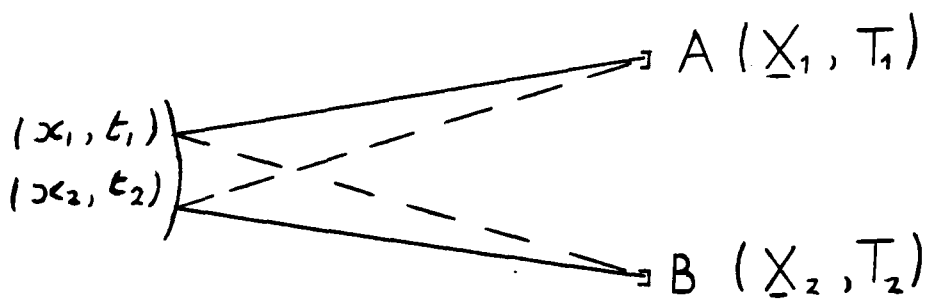

Figure 1. Diagram of the HBT Effect

Let two particles be randomly emitted from the source at space-time points $(\underline{x}_1,t_1)$, $(\underline{x}_2,t_2)$, and at a later time a coincidence be registered in the two detectors A and B situated at $(\underline{X}_1,T_1)$ and $(\underline{X}_2,T_2)$, $(T_1 \simeq T_2)$. Because of the path ambiguity we do not know whether the particle detected by A came from $\underline{x}_1$ or $\underline{x}_2$, similarly for that detected by B. Hence the total

amplitude for detecting two bosons (fermions) in the sum (difference) of the amplitudes for each path.

The probability of detecting a coincidence is the square of this sum,

$$\text{prob } a \left| e^{i\underline{k}_1\cdot(\underline{X}_1-\underline{x}_1)\ -iE_1(T_1-t_1)}\ e^{i\underline{k}_2\cdot(\underline{X}_2-\underline{x}_2)\ -iE_2(T_2-t_2)}\right.$$

$$\left. \pm\ e^{i\underline{k}_1\cdot(\underline{X}_1-\underline{x}_2)\ -iE_1(T_1-t_2)}\ e^{i\underline{k}_2\cdot(\underline{X}_2-\underline{x}_1)\ -iE_2(T_2-t_1)}\right|^2 \quad (1)$$

E_i, k_i are the energy and wave-vector for the particle detected at X_i, and the upper sign refers to bosons, the lower to fermions.

Equation 1 may be rewritten as

$$P(\underline{X}_1T_1,\ \underline{X}_2T_2) = 1 \pm \cos(\underline{q}.\underline{r} - Et) \quad (2)$$

where
$$\begin{aligned} \underline{q} &= \underline{k}_1-\underline{k}_2 \\ E &= E_1-E_2 \\ \underline{r} &= \underline{x}_1-\underline{x}_2 \\ t &= t_1-t_2 \end{aligned}$$

We see that an interference pattern results which depends essentially on the size of the source. The interference pattern is seen by varying the angular separation of the detectors, and hence varying $\underline{q}$. So far we have assumed two point sources, let us now assume a normalized distribution function $D(\underline{x},t)$ for the emission of a particle at $(\underline{x},t)$. The two-particle joint probability distribution function is obtained by integrating the product of the distribution functions for the emission of two particles and the probability of detecting a coincidence over

the coordinates of the source. The correlation function is defined as the ratio of the joint probability to the square of the single-particle probability. If the single-particle distribution function is normalised so that its integral over all space-time is unity the correlation function is given by

$$C_2(\underline{X}_1T_1,\underline{X}_2T_2) = \int d^3x_1 d^3x_2\, dt_1 dt_2\, D(\underline{x}_1 t_1)\, D(\underline{x}_2 t_2)$$

$$\times\, P(\underline{X}_1T_1,\underline{X}_2T_2) \qquad (3)$$

For example, consider a Gaussian distribution function

$$D(\underline{x},t)\ \alpha\ e^{-x^2/r_0^2\ -\ t^2/\tau^2}$$

where r_0, τ are measures of the spatial and temporal extent of the source. The correlation function is now

$$C_2\ (\underline{X}_1T_1,\ \underline{X}_2T_2) = 1 \pm e^{-q^2r_0^2/2\ -\ E^2\tau^2/2} \qquad (4)$$

We have plotted C_2 (for $\tau=0$) in Figure 2.

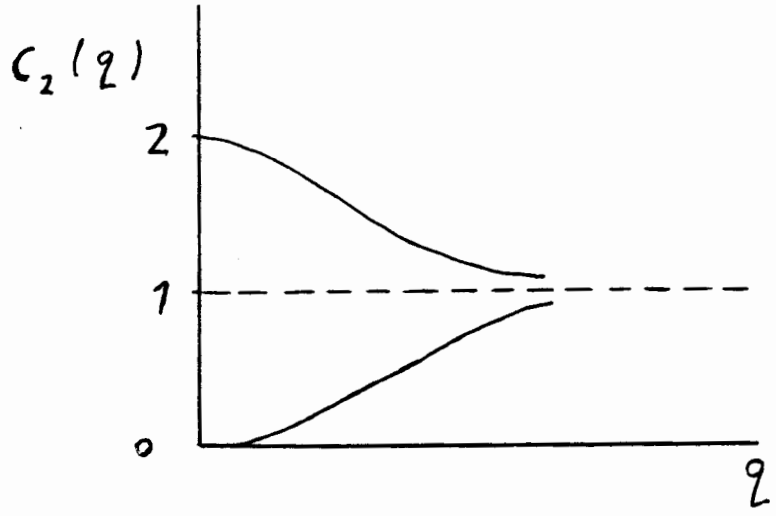

Figure 2: Two-Particle Correlation Function

The upper curve applies to bosons, the lower to fermions. For both types of particle the two-particle correlation function becomes 1 at large $\underline{q} = \underline{k}_1 - \underline{k}_2$. This expresses the fact that the two-particle joint probability goes over to the square of the single-particle probability when the events are independent, i.e. as the two particles diverge in momentum. There is an enhanced probability of finding two bosons with equal momenta, i.e. $\underline{q}=0$, whilst the probability for detecting two such fermions is zero because of the Pauli exclusion principle. We note that the effect depends essentially on the path ambiguity, and this in turn means that the particles must satisfy the "uncertainty relation" $\Delta\underline{p}\cdot c\Delta t \leq \hbar$ where $\Delta\underline{p}$, Δt are the differences between

the two particles' momenta and times of emission. This brings out the fact that if the particles are widely separated in time or space their statistics are not important.

From equation 4 we may determine the spatial and temporal extent of the Gaussian emitting region, by relating the correlation function to the two-particle and single-particle inclusive cross-sections measured in experiments. We define this relation by

$$\frac{d^2\sigma}{d\underline{p}_1 d\underline{p}_2} = \frac{d\sigma}{d\underline{p}_1}\,\frac{d\sigma}{d\underline{p}_2}\,C_2(\Delta\underline{p}) \qquad (5)$$

where $\Delta\underline{p}$ is the relative momentum of the two particles.

With this definition we see that the two-particle inclusive cross-section becomes the square of the single particle cross-section as the particles move apart in phase space. This is expected because two particles with widely different momenta or energies are independent.

We see from this simple calculation that a measurable effect exists and that the rate of two-particle coincidences is twice the random rate at zero relative momentum for bosons, and zero for fermions. These results are not drastically changed by the inclusion of final state interactions between the particles although the calculation becomes considerably more complicated than the simple derivation presented here.

2. Reaction Mechanisms in Heavy Ion Collisions

2.1 Introduction

In collisions involving two heavy ions the large number of participating nucleons implies that several different mechanisms may contribute to the reaction mechanism which are absent in free nucleon-nucleon (NN) collisions. There is still the analogue of the free NN process, where each nucleon undergoes at most one significant collision, although it may be modified by the presence of the residual nucleus. At the other extreme there is the possibility of each nucleon in the projectile undergoing many successive collisions and giving up its energy to a large number of nucleons which form a thermally equilibrated system. This region of 'hot' nuclear matter then cools down gradually as it expands and breaks up into fragments. To distinguish these two processes we define the nucleon mean free path λ, and the mean linear dimension of the system R. The mean free path is the average distance betwen successive NN collisions.

In the next two sections we discuss the two extreme pictures of HI collisions: as a superposition of many free NN collisions, and as the formation of a hot, dense region of nuclear matter due to multiple scattering of the participating nucleons. As we shall see most of the inclusive data are not well described by either of these pictures alone but fall somewhere in the middle. However the formation of a region of

hot nuclear matter is supported by some recent experimental evidence based on a hydrodynamic approach.

2.2 Direct Limit

For the nucleons inside the projectile to undergo only one collision the mean free path λ must be much greater than the linear dimension R. This is called the direct limit. Obviously, it will lead to reaction products, and hence inclusive spectra, similar to free NN collisions. However the presence of the residual nucleus cannot be ignored. In a free elastic NN collison the energy of the projectile is shared between the two particles. There is thus an allowed range of energies for each particle from zero up to the total beam energy. In HI Collisions where the two nucleons are embedded in large nuclei this simple two-body scattering picture is obscured by the fact that the residual nucleus can leave with a large momentum though small energy. The energy and momentum of the ejectile may thus be very large, e.g. the emission of a high transverse momentum proton. This leads to a larger amount of phase space available to the ejectiles than is possible in the free NN process. Another new effect is due to the fermi motion of the nucleons inside the two nuclei. If we treat the nucleus as an ideal gas of fermions, then the Pauli exclusion principle will cause the nucleons to fill up the lowest energy states. There will be a maximum ground-state energy, called the fermi energy, of the order of

tens of MeV for heavy nuclei. Nucleons much below the fermi surface cannot participate in scattering through large angles as there is no empty state for them to go into. However if they gain enough energy to jump above the fermi surface they can interact. There is a certain minimum momentum necessary for a particle to scatter through a large angle. Because of this the quasielastic scattering peak will be reduced at large angles, where the energy of the particles is small. We can see this effect in Figure 3, which shows data from protons on ^{12}C from Tanihata et al.[14 15] At small angles a peak due to pp or pn quasi-elastic scatterings is visible and the energy of the ejectile is large. As we go to larger angles the energy of the particle drops and the peak becomes lost in the background. The fermi motion of the nucleons inside the nuclei effectively smears out the quasi-elastic scattering peak. This peak also disappears as the projectile and target mass increase reflecting the greater importance of multiple scattering for such systems. The relative importance of the direct component in heavy ion collisions may be determined from large-angle two-proton correlations.[14 15] In these experiments the ratio of in-plane coincidences to out-of-plane coincidences is measured. This ratio should be near one if the thermal process is dominant as the emission of particles is then random. However, if the direct limit applies this ratio should be larger than one because pp quasi-elastic scatterings tend to produce two protons in the same reaction plane. It is found that the ratio is larger than

one and shows a peak at the momentum expected from quasi-elastic pp scattering, although the data show that only about one sixth of the protons emitted are from direct processes which suggests that the direct component is watered down by the presence of multiple scattering of the nucleons.

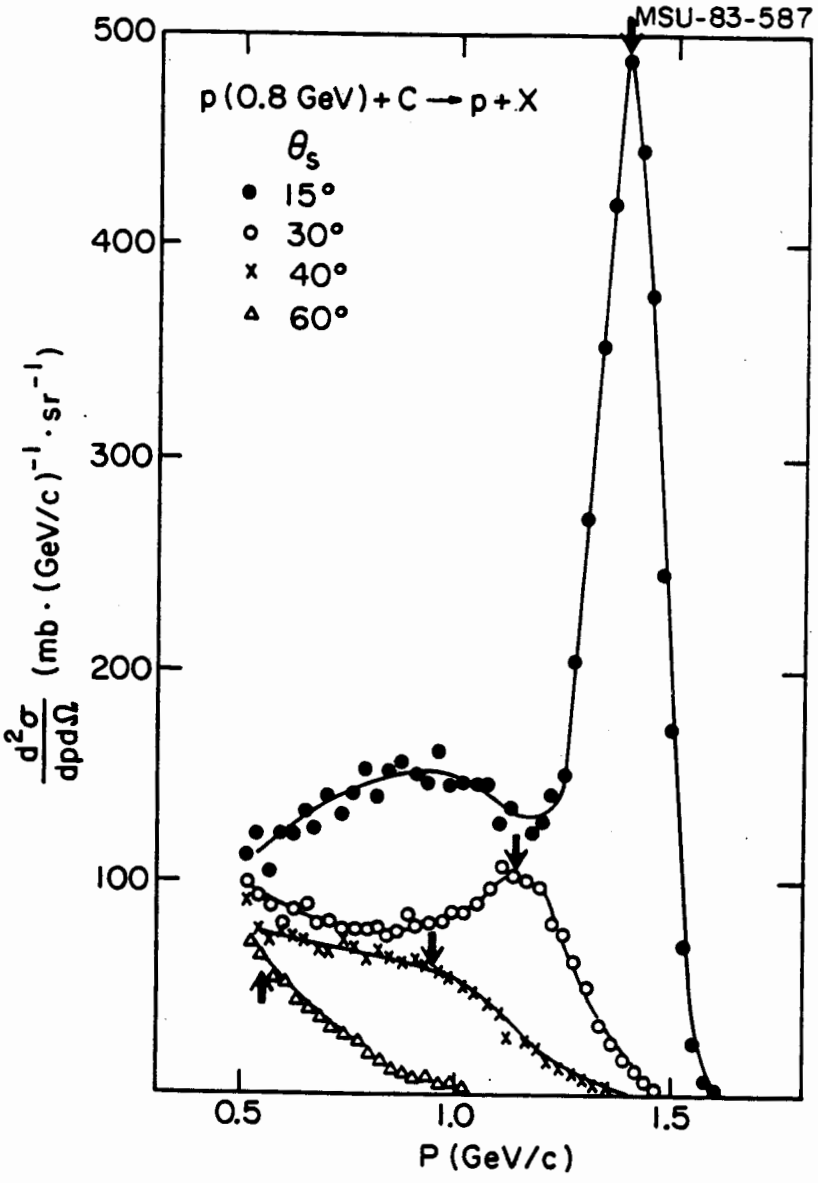

Figure 3. Inclusive proton spectra from p+C collisions at a beam energy of 800 MeV. The arrows indicate the momenta expected from pp or pn quasielastic scatterings. Figure from Ref. 27

We turn now to a determination of the proton mean free path in HI collisions from pp coincidence experiments.[14] [15]

In Figure 4a the target mass dependence of the single proton quasi-elastic scattering yield is shown, and Figure 4b shows the dependence of the two-proton in-plane coincidence yields from pp quasi-elastic scattering. The single proton inclusive yields are easily calculated at forward angles as the data are strongly forward peaked. The yields are proportional to $A^{1/3}$, where A is the target mass number. Figure 4b shows that the coincidence cross-section increases with mass up to A=50 and then decreases. This is to be expected as the probability of NN scattering increases with mass but so also does the probability of subsequent rescattering of one of the particles. If either of the two particles is rescattered the coincidence is of course destroyed.

By relating the probability of rescattering to the proton mean free path, a fit to the data yielded a value of λ=2.4 fm. This is somewhat larger than is expected from free NN collisions, a fact due to the strong forward peaking of the elastic scattering at the energies involved, where the nucleons may undergo collisions which do not significantly alter their momenta, causing the mean free path to appear larger than it really is.

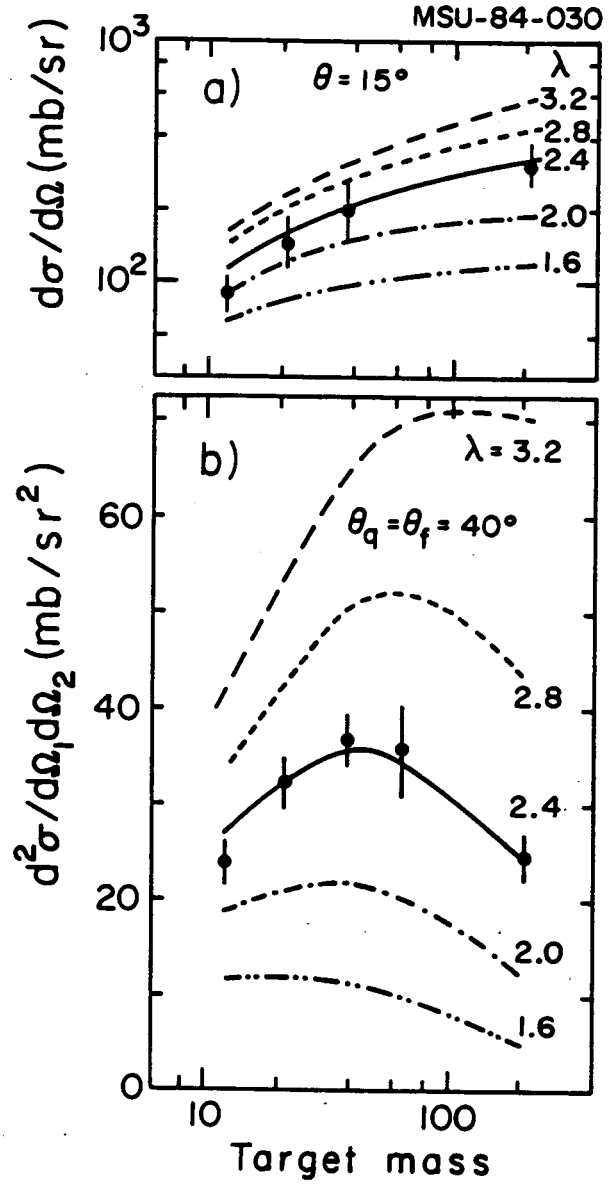

Figure 4. Target-mass dependence of (a) inclusive proton and (b) two-proton quasielastic scattering cross-sections. Figure from Ref. 27.

2.3 Thermal Limit

It has been found that even for light targets a significant amount of multiple scattering takes place.[16] This suggests that the projectile's energy will be shared among all the nucleons within a certain region. If the interaction time is long enough this region may reach thermal equilibrium and provide an example of very hot, dense nuclear matter. The question of whether thermal equilibrium is actually reached in HI reactions is still open. The approach to thermal equilibrium has been investigated in the so-called fireball model.[17] [18] In its original form this model proposed that the projectile sweeps out a cylindrical region of the target nucleus leaving a spectator region from the target, and, if the impact parameter is large enough, also one from the projectile. The swept out nucleons form a thermally equilibrated system which then decays as an ideal Fermi gas. The properties of the fireball, i.e. the number of swept out nucleons, the laboratory velocity of the centre of mass and its energy can all be calculated as a function of the impact parameter. In calculating the temperature of the fireball it is assumed that the available energy per nucleon is the incident CM energy minus the binding energy. It is assumed that this energy heats up the nucleons leading to a quasi-equilibrated region - the "fireball". This fireball is then treated as a relativistic ideal gas, whose temperature depends on the available energy per nucleon, which cools down emitting protons and light particles.

Using the fireball model, Westfall et al.[17] were able to fit the proton inclusive spectra from the reactions ^{4}He and ^{20}Ne on ^{238}U at 250 MeV/Nucleon and 400 MeV/Nucleon. Good agreement with the data was found. However for the higher energy reaction ^{20}Ne on ^{238}U at 2100 MeV/Nucleon, the model failed to describe the data. It was necessary in the fireball calculation to assume that almost all the initial CM kinetic energy of the projectile went into heating up the system. This produced good agreement with the low energy data but for the high energy reaction the temperature and velocity of the fireball were too high. If it was assumed that only about one quarter of the initial energy went into heating up the fireball then agreement with the data could be restored. The authors tried to explain this by assuming that two fireballs were produced in very high energy reactions. They also pointed out that the success of such a simple model at low energies suggests the importance of using thermodynamic concepts in relativistic HI reactions. The large number of nucleons involved and multiple scattering of the particles leads to a thermally equilibrated region which may be described using the language of equilibrium thermodynamics.

With this indication that thermalisation is partially achieved in HI reactions, one may use the small-angle two-particle coincidence measurements described in Chapter 1 to measure the size of the thermally equilibrated region. The results of these experiments with protons and pions suggest a value for the radius of a Gaussian source of 3-5 fm. [5-11]

2.4 The Hydrodynamic Model

A final example of the application of semi-classical models to HI reactions is the hydrodynamic model.

The thermal model assumes a short mean free path for nucleons inside the nucleus and a long interaction time and treats the reaction as a hot, dense system of nucleons in thermal equilibrium. However it does not make any specific assumptions as to how the system reaches this equilibrium state. The hydrodynamic model also assumes a very short mean free path and a long interaction time but makes the assumption that the nuclei can be treated as drops of an ideal fluid. The idea of treating nuclei as drops of a classical, incompressible liquid was first put forward forty years ago by Von Wëizsacker[19] when proposing the semi-empirical mass formula. He treated a nucleus as a drop of liquid with energy terms due to the volume, surface tension, Coulomb energy of the protons, etc. In a collision, one basically assumes that the nuclei are incompressible and hence must either bounce off one another or break up. For small impact parameter collisions we expect the nuclei to break up due to the large energy transfer while for peripheral collisions we expect them to bounce off one another.

Data from some recent experiments[20] seem to show this type of behaviour. From the reaction $^{20}Ne + ^{238}U$ at beam energies of 393 MeV/A the high multiplicity events (presumably from small impact parameter collisions) show no signs of the strong forward

peaking seen in low multiplicity events and expected from cascade or thermal models. There is instead a broad peak in the cross-section for low energy protons at lab angles of 70°-90°. Stöcker et al[21 22] have interpreted this broad peaking as the result of the hydrodynamical side-splash. At small impact parameters a large part of the target nucleus is pushed forward by the projectile nucleus. The non-overlapping parts of the target however receive a sideward push from the collision. This sidewards push should show up in the low energy fragments as it happens mainly in the spectator regions of the target.

Another hydrodynamic effect is seen in the pp coincidence data taken from the same experiment. It was found that if a fast proton was detected at 40° to the beam then the coincidence rate for another fast proton on the same side or a slow proton on the opposite side of the beam was increased above the background. This suggests that the fast protons came from the projectile nucleus which 'bounced off' the target (in a large impact parameter collision) while the slow protons came from the target nucleus which was pushed in the opposite direction.

Hydrodynamic behaviour of nuclei in heavy ion collisions is still a speculative topic, especially as the principal condition of a short mean free path ($\lambda<R$) is not likely to be satisfied. The results seem to indicate that hydrodynamic effects contribute perhaps 10-30% of the reaction products.

3. The Nuclear Hanbury-Brown Twiss Effect

3.1 Introduction

In section 1.2 we derived a simple case of the HBT effect for two particles where we ignored all final state interactions (FSI) so the correlation was due only to the particles' boson or fermion nature. This is justifiable if the particles are weakly interacting, as, for example for photons from a star, but not for particles emitted in a HI collision. For pion emission the Coulomb interaction is generally corrected for by using the standard Gamow factor[5-8]

$$G(\nu) = \frac{2\pi\nu}{e^{2\pi\nu} - 1} \qquad \nu = \frac{\mu e^2}{\hbar^2 k} \tag{6}$$

where ν is the Sommerfeld parameter. This is approximately the modulus squared of the wave function for relative motion of the two particles as their distance apart goes to zero, and is a measure of the attraction or repulsion of the interaction between the particles. For protons and heavier fragments this correction is not sufficient, and the interaction of the particles, via the strong nuclear force and Coulomb force, must be taken into account directly by calculating their effect on the trajectories of the emitted fragments. Qualitatively, we expect that two identical charged particles emitted within the

range of the strong nuclear force will be drawn together (assuming an attractive potential) whilst the repulsive Coulomb force will prevent them ever having precisely equal final momenta. This should lead to an enhancement in the number of coincidences at small relative momenta although the Coulomb repulsion will cause the number of coincidences to drop to zero as the relative momentum goes to zero. Defining the correlation function $R(\underline{p}_1,\underline{p}_2)$ to be the ratio of the two-particle inclusive cross-section to the square of the single particle inclusive cross-section

$$\frac{d^2\sigma}{d\underline{p}_1 d\underline{p}_2} = \left[\frac{d\sigma}{d\underline{p}}\right]^2 (1+R(\underline{p}_1,\underline{p}_2)) \qquad (7)$$

We expect R to be -1 at $\underline{p}_1=\underline{p}_2$, rise to a positive peak for small values of relative momentum and fall to zero as $|\underline{p}_1-\underline{p}_2|$ increases further. In this section we derive an expression for the correlation function including the effects of final state interactions. These are seen to alter the correlation function from its form due to statistics alone, and this alteration follows the simple picture given above. We derive it first for the case of a Gaussian source in both space and time and then for the case of a δ-function distribution in space keeping the Gaussian time dependence. Finally we extend the derivation to two-deuteron and two-triton correlation functions with negligible source lifetimes.

3.2 The Two-Proton Correlation Function

3.2.1 PP Correlation Function with Negligible Source Lifetime

We describe here the calculation first derived by Koonin[13] of the two-proton correlation function. We consider a source volume in an HI collision which emits protons evenly over its surface, with random spin alignments. Let $D(\underline{r},t,\underline{p})$ be the distribution function for producing a proton of momentum $\underline{p}$ at space-time point $(\underline{r},t)$. D is normalized by taking its integral over all space-time to be equal to the single proton differential cross-section divided by the total proton inclusive cross-section

$$\int D(\underline{r},t,\underline{p})\, d^3r\, dt = \frac{1}{\sigma}\frac{d\sigma}{d\underline{p}} \qquad (8)$$

Let two protons be emitted at space-time points $(\underline{r}_1,t_1)$, $(\underline{r}_2,t_2)$ with equal momenta $\underline{p}$, and $t_2 \geq t_1$. Then at time t_2 the first proton is at $\underline{r}_1' = \underline{r}_1 + \underline{V}(t_2-t_1)$, where $\underline{V} = \underline{P}/M$ is the laboratory velocity of the pp centre of mass, $\underline{P}=\underline{p}_1+\underline{p}_2$ is the total momentum and $M = 2m_p$. The probability of observing two protons with momenta $\underline{p}_1 \simeq \underline{p}_2 \simeq \underline{p}$, is then the modulus squared of the wave function for two protons at $\underline{r}_1'$, $\underline{r}_2$. Since two protons may combine to form a spin 0 or spin 1 state, with statistical weights 1/4, 3/4 respectively, we must add the probabilities of each state. After considering the case $t_1 \geq t_2$ as well, the

two-proton inclusive cross-section is given by

$$\frac{1}{\sigma}\frac{d^2\sigma}{d\underline{p}_1 d\underline{p}_2} = \int dt_1\, dt_2\, d^3r_1\, d^3r_2\, D(\underline{r}_1,t_1,\underline{p})\, D(\underline{r}_2,t_2,\underline{p})$$

$$\times \{ \tfrac{1}{4}|{}^0\Psi(\underline{r}_1', \underline{r}_2)|^2 + \tfrac{3}{4}|{}^1\Psi(\underline{r}_1', \underline{r}_2)|^2\} \qquad (9)$$

where ${}^0\Psi$, and ${}^1\Psi$ are the singlet and triplet pp scattering wave functions, which are respectively symmetric and anti-symmetric under interchange of the two particles, and satisfy the time independent two-body Schrödinger equation with nuclear and Coulomb potentials.

We have neglected the influence of the nuclear mean field on the two protons and so the scattering wave function is the product of a plane wave for CM motion and the wave function for relative motion. The former depends only on the total momentum and CM position, $\underline{R} = (\underline{r}_1' + \underline{r}_2)/2$, and the latter only on the relative momentum $\Delta\underline{p} = (\underline{p}_1 - \underline{p}_2)/2$, and relative position $\underline{r}' = \underline{r}_1' - \underline{r}_2$.

We now assume a Gaussian shape in space and time for the distribution function, with the normalisation condition given in equation 8,

$$D(\underline{r},t,\underline{p}) = \frac{1}{\sigma}\frac{d\sigma}{d\underline{p}}\frac{1}{\pi^2 r_0{}^3 \tau}\, e^{-(\underline{r}-\underline{V}_0 t)^2/r_0{}^2}\, e^{-t^2/\tau^2} \qquad (10)$$

The parameters r_0, τ are the Gaussian radius and lifetime of the region producing protons, $\underline{V}_0$ is the laboratory velocity of this region taken to lie along the beam direction. We have used $(\underline{r}-\underline{V}_0 t)$ because in general we expect the source volume to move with a non-zero velocity rather than being at rest as was tacitly assumed before. Equation 10 is now inserted into equation 9, together with the wave functions and the integral evaluated as far as possible. We show the calculation in Appendix A, here we just state the result. The two-proton correlation function $R(\underline{p}_1, \underline{p}_2)$ is given by

$$1 + R(\underline{p}_1, \underline{p}_2) = \frac{1}{(2\pi)^{3/2} r_0^2 \rho} \int d^3r \; e^{-[r^2 - (\underline{r}\cdot\underline{V'}\,\tau/\rho)^2]/2r_0^2} \times \{\tfrac{1}{4}|{}^0\Psi(\underline{r}, \Delta\underline{p})|^2 + \tfrac{3}{4}|{}^1\Psi(\underline{r}, \Delta\underline{p})|^2\} \qquad (11)$$

where $\underline{V}' = \underline{V} - \underline{V}_0$, $\rho^2 = r_0^2 + (V'\tau)^2$, and the wave functions are now the anti-symmetrised solutions of the Schrödinger equation for relative motion of two protons. Equation 11 must be evaluated numerically. The wave functions are expanded in a partial wave series and the Coloumb potential is used in all partial waves. The nuclear potential is used only in the S-wave as the short-range nuclear force is only effective in correlating protons with relative momenta $\Delta p \leq 40$ MeV/c.

In evaluating equation 11 we treat several cases. For simplicity we first derive the $\tau=0$ limit of the correlation function. This case describes collisions which emit particles

over a finite spatial region but with a negligible lifetime.

With $\tau=0$, equation 11 becomes

$$1 + R(\underline{p}_1,\underline{p}_2) = \frac{1}{(2\pi)^{3/2} r_0^3} \int d^3r\, e^{-r^2/2r_0^2}$$

$$\times \tfrac{1}{4}\{|{}^0\Psi(\underline{r}, \Delta\underline{p})|^2 + \tfrac{3}{4}|{}^1\Psi(\underline{r}, \Delta\underline{p})|^2\} \qquad (12)$$

To evaluate this we need to know the singlet and triplet wave functions for relative motion. The Schrödinger equation for the relative motion of two protons, with reduced mass $\mu = \frac{1}{2}m_p$, moving under the influence of their mutual coloumb and nuclear forces, is

$$\{\frac{-\hbar^2}{2\mu}\nabla^2_{\text{Rel}} + \frac{e^2}{r} + V_{\text{nuc}}(\underline{r}) - E\}\Psi = 0 \qquad (13)$$

If $V_{\text{nuc}}(\underline{r}) = 0$ we obtain as the solutions the so-called Coulomb wave functions which are written in terms of a partial wave expansion as

$$\Psi(\underline{r}) = \sum_L \Phi_L(kr) P_L(\cos\theta) \qquad (14)$$

$$\Phi_L(kr) = e^{-\nu\pi/2} \frac{\Gamma(L+1+i\nu)(2ikr)^L}{(2L)!} e^{ikr} \, {}_1F_1(L+1+i\nu, 2L+2; -2ikr) \tag{15}$$

where $\Gamma(Z)$ is the complex gamma function, $\nu = \mu e^2/\hbar^2 k$ is the Sommerfeld parameter, and ${}_1F_1(a,c;z)$ is the confluent hypergeometric function given by the series expansion

$${}_1F_1(a,c;Z) = 1 + \frac{aZ}{c} + \frac{a(a+1)}{c(c+1)} \frac{Z^2}{2!} + \ldots \tag{16}$$

The solution, equation 15, is obtained by solving the Schrödinger equation in spherical polar coordinates and equating the asymptotic form of the solution as $r \to \infty$ to the solution in parabolic coordinates. We choose the normalization such that the solution behaves as a plane wave in the absence of the coulomb interaction and goes over to a plane wave asymptotically as $r \to \infty$.

Now two protons may combine to give states of total spin S=0 or 1 which are respectively anti-symmetric and symmetric under interchange of the two spins. The total wave function for relative motion is thus composed of a product of a spin part and a space part

$$\Psi_{rel} = \Psi_{space}(\underline{r})\ \chi_{spin}(1,2) \qquad (17)$$

In order that the total wave function be anti-symmetric under interchange of the two protons, as required by the Pauli exclusion principle, the anti-symmetrised form of equation 17 must be used, denoting the total spin by a superscript

$$^{0}\Psi_{Rel} = \frac{1}{\sqrt{2}}\{\Psi_{space}(\underline{r}) + \Psi_{space}(-\underline{r})\}\ ^{0}\chi(1,2)$$

$$^{1}\Psi_{Rel} = \frac{1}{\sqrt{2}}\{\Psi_{space}(\underline{r}) - \Psi_{space}(-\underline{r})\}\ ^{1}\chi(1,2)$$

where $^{0}\chi$ is anti-symmetric and $^{1}\chi$ symmetric under an interchange of their spin arguments. Assuming normalized spin eigenfunctions (which will drop out on taking the modulus squared of the probability amplitude), we may write the anti-symmetrised solutions of equation 13 as

$$\Psi_{Rel} = \frac{1}{\sqrt{2}}\{\Sigma_{L}\ \Phi_{L}(kr)P_{L}\cos(\theta) \pm \Sigma_{L}\ \Phi_{L}(-kr)P_{L}(\cos\theta)\}$$

where the upper sign refers to the singlet case, the lower to the triplet, and the summation is over all partial waves. Now $\underline{r}\rightarrow-\underline{r}$ is equivalent to $\theta\rightarrow\pi-\theta$, $\phi\rightarrow\pi+\phi$ and there is no ϕ dependence, also

$$P_{L}(\cos(\pi-\theta)) = (-1)^{L}\ P_{L}(\cos\theta)$$

and so

$$ {}^{0}\Psi_{Rel} = \sqrt{2} \sum_{L\ even} \Phi_L(kr)\, P_L(\cos\theta) \qquad (18a) $$

$$ {}^{1}\Psi_{Rel} = \sqrt{2} \sum_{L\ odd} \Phi_L(kr) P_L(\cos\theta) \qquad (18b) $$

We shall use the abbreviation in this section that

$$ \Sigma' = P_s \sum_{L\ even} + P_t \sum_{L\ odd} $$

denotes P_s times the sum over even L plus P_t times the sum over odd L, where $P_s = 1/4$, $P_t = 3/4$ are the statistical weights of the singlet and triplet states respectively. The correlation function may now be written

$$1 + R(\underline{p}_1,\underline{p}_2) = \frac{1}{(2\pi)^{3/2} r_0^3} \int d^3r \, e^{-r^2/2r_0^2}$$

$$\times \{\sqrt{2}\, \Sigma' \, \Phi_L(kr)\, P_L(\cos\theta)\}^2$$

$$= \frac{1}{(2\pi)^{1/2} r_0^3} \int_0^\infty \int_0^\pi r^2 \, e^{-r^2/2r_0^2} \, dr \sin\theta \, d\theta$$

$$\times [2\, \Sigma' \, \Phi^*_L \Phi_{L'} \, P_L(\cos\theta) P_{L'}(\cos\theta)] \qquad (19)$$

The summation over L is bounded as it is just the wave function for relative motion and vanishes at infinity. Interchanging the order of the sum and integral over θ and using the orthogonality of Legendre Polynomials gives

$$1 + R(\underline{p}_1,\underline{p}_2) = \frac{2}{(2\pi)^{1/2} r_0^3} \int_0^\infty dr \, r^2 \, e^{-r^2/2r_0^2}$$

$$\times \{\, \Sigma' \, |\Phi_L|^2 \, \frac{2}{2L+1}\} \qquad (20)$$

Equation 20 now has to be evaluated numerically. To calculate the wave functions we use the Couloumb potential and Reid Soft-core nuclear potential for the S-wave, and the Coulomb potential only for higher partial waves.

The S-wave was calculated by numerically integrating Schrödinger's equation; the higher partial waves were evaluated

from the series solution, equation 15, and the asymptotic form of this solution for large values of kr.

The correlation function was calculated on a computer, with the lifetime τ set equal to zero, using the programme CORFUN10 in Appendix B. Figures 5a-c show the two proton correlation function plotted against relative momentum for several values of r_0 (with τ=0). The data are taken from experiments performed at Michigan State University and Oak Ridge [23] for Au, Al and C targets bombarded by 400 MeV O ions.

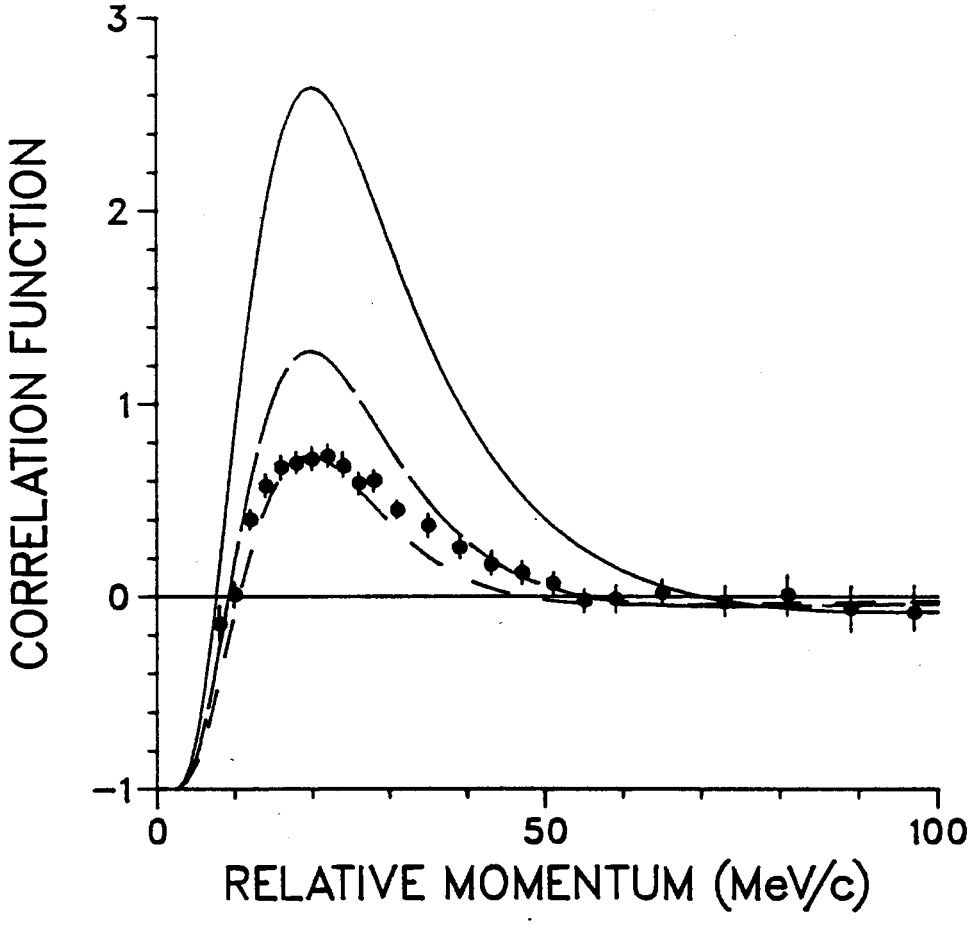

Figure 5a. Two-proton correlation function, $R(\underline{P}_1,\underline{P}_2)$, for a source with Gaussian equivalent radius r_0 and zero lifetime. The data are for the reaction $^{197}Au(^{16}O,pp)X$ from Ref. 23. The curve labels are: r_0=2.0 fm ————, r_0=3.0 fm—— ——, r_0=3.7 fm— — —.

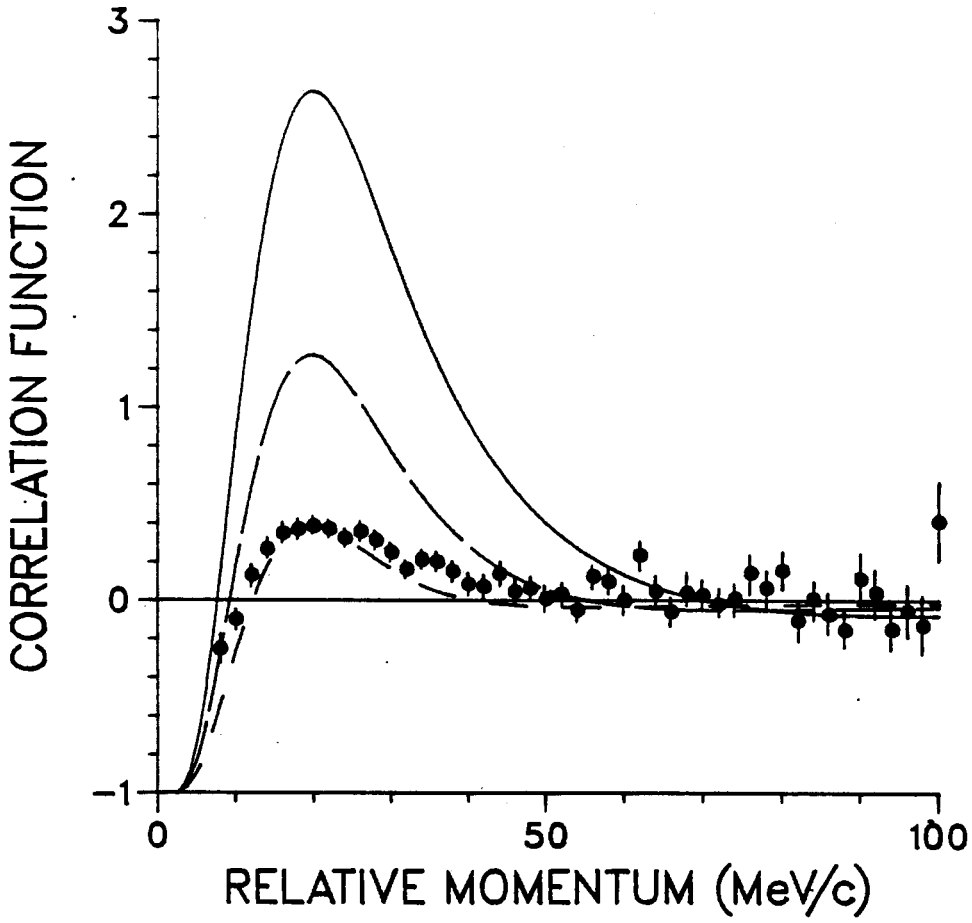

Figure 5b. Two-proton correlation function, $R(\underline{P}_1,\underline{P}_2)$, for a source with Gaussian equivalent radius r_0 and zero lifetime. The data are for the reaction $^{27}Al(^{16}O,pp)X$ from Ref. 23. The curve labels are: r_0=2.0 fm ———— , r_0=3.0 fm —— ——, r_0=4.7 fm— — —.

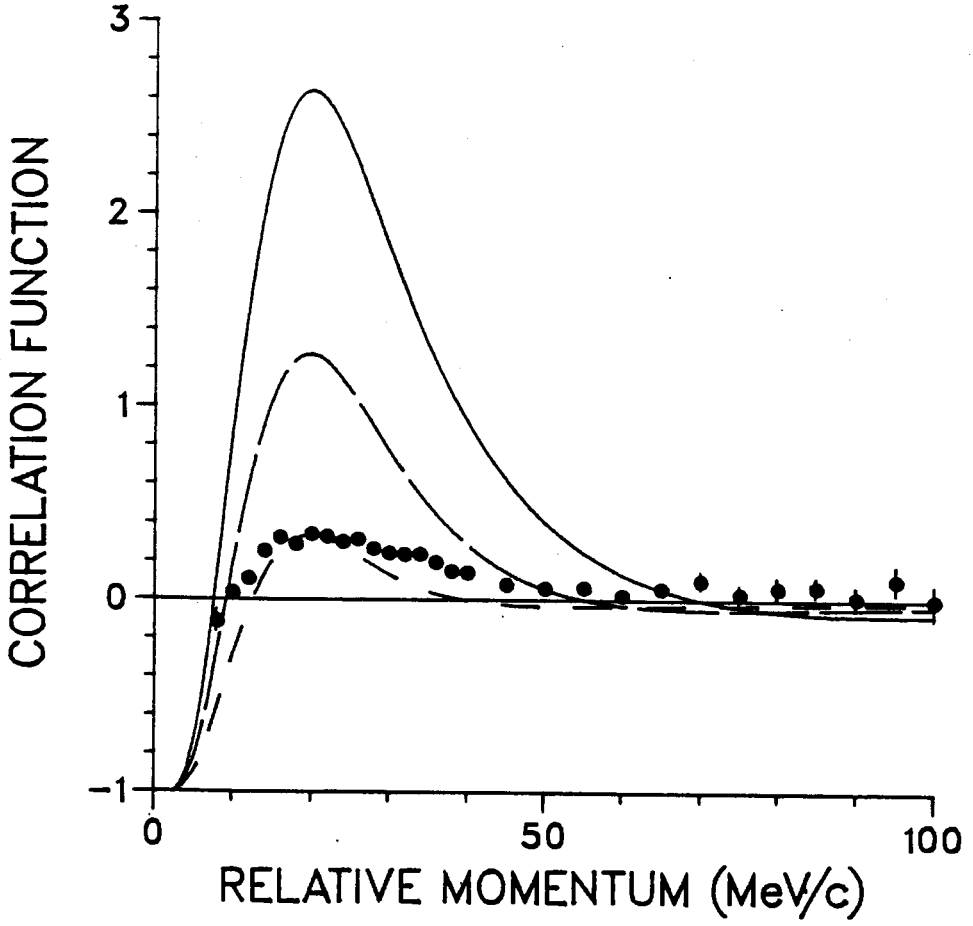

Figure 5c. Two-proton correlation function, $R(\underline{P}_1,\underline{P}_2)$, for a source with Gaussian equivalent radius r_0 and zero lifetime. The data are for the reaction $^{12}C(^{16}O,pp)X$ from Ref. 23. The curve labels are: r_0=2.0 fm————————, r_0=3.0 fm———— ———— , r_0=4.9 fm— — — —.

From the figures it can be seen that the nuclear force causes a large peak in the correlation function at $\Delta p \simeq 20$ MeV/c. The peak drops with increasing r_0 as the short-range nuclear force cannot affect two protons far apart in space. The peak height also decreases with decreasing target mass, we shall return to this point in Chapter 4.

To close this section, it is worthwhile to look at some limiting cases of the $\tau=0$ correlation function. Firstly, we present the case where the particles have no interactions except their statistics, i.e. bosons or fermions, and secondly, we take the limit as the relative momentum goes to zero keeping the Coulomb interaction only.

a) Correlation Function with no FSI:

In this case the wave function for relative motion is just a plane wave, the correctly symmetrised singlet and triplet wave functions are then

$$\Psi_s \simeq \frac{1}{\sqrt{2}} \left(e^{i\underline{k}\cdot\underline{r}} + e^{-i\underline{k}\cdot\underline{r}}\right) = \sqrt{2}\cos(\underline{k}\cdot\underline{r}) \qquad (21a)$$

$$\text{as} \quad \Psi \simeq \frac{1}{\sqrt{2}} \left(e^{i\underline{k}\cdot\underline{r}} - e^{-i\underline{k}\cdot\underline{r}}\right) = \sqrt{2}i\sin(\underline{k}\cdot\underline{r}) \qquad (21b)$$

so equation 12 becomes

$$1 + R(\underline{p}_1,\underline{p}_2) = \frac{1}{(2\pi)^{3/2}r_0^3}\int d^3r\, e^{-r^2/2r_0^2}\{\tfrac{1}{4}|{}^{s}\Psi|^2 + \tfrac{3}{4}|{}^{as}\Psi|^2\}$$

$$= \frac{1}{(2\pi)^{3/2}r_0^3}\int d^3r\, e^{-r^2/2r_0^2}\{1-\tfrac{1}{2}\cos(2\underline{k}\cdot\underline{r})\} \qquad (22)$$

Evaluating the 3 dimensional Gaussian integral gives

$$R(\underline{p}_1,\underline{p}_2) = -\tfrac{1}{2}\, e^{-2k^2 r_0^2} \qquad (23)$$

Comparing this result with the simple case derived in Section 1.3, (recalling the relation $C_2 = 1 + R(\underline{p}_1,\underline{p}_2)$) we see that the effect of the statistics is just the numerical factor in front of the exponential. Taking the limit as k goes to 0 of equation 23 just gives $R(\underline{p}_1,\underline{p}_2) = -1/2$. By setting all the potentials equal to zero in the programme CORFUN10 the limit given by equation 23 was found.

b) Correlation Function with Couloumb Interaction Only as k -> 0

Returning to the definition, equation 12

$$1 + R(\underline{p}_1,\underline{p}_2) = \frac{1}{(2\pi)^{3/2}r_0^3}\int d^3r\, e^{-r^2/2r_0^2}\{\tfrac{1}{4}|{}^{0}\Psi|^2 + \tfrac{3}{4}|{}^{1}\Psi|^2\}$$

We make a partial wave expansion of the Coulomb wave functions as before and note that as the relative momentum goes to zero the only partial wave which remains non-zero is the S-wave, which goes over to the Gamow factor

$$\lim_{kr\to 0} |\Phi_0(kr)|^2 = \frac{2\pi\nu}{e^{2\pi\nu} - 1} \tag{24}$$

where ν is the Sommerfeld parameter. In the limit as k approaches zero, ν goes to infinity and hence the wave vanishes. Thus the correlation function is just

$$\lim_{k\to 0} R(\underline{p}_1, \underline{p}_2) = -1 \tag{25}$$

This expresses the fact that the long-range Coulomb force prevents two protons from ever having precisely equal final momenta regardless of when or where they were emitted.

Comparing equations 23 and 25 we see that in the absence of any FSI two protons can have identical momenta as long as they have opposite spin. Once the Coulomb force is turned on two protons can never have exactly the same momentum and a complete anti-correlation results.

3.2.2 Series Expansion For the pp Correlation Function

The pp correlation function defined in terms of an integral, equation 11, can only be evaluated numerically. However the case of negligible source lifetime (τ=0) is much easier to evaluate than the corresponding non-zero lifetime case. Here we evaluate the correlation function for finite τ by expanding the exponential involving $V'\tau$ as a Taylor Series and integrating term by term. We leave to the next section a more elegant way of finding an upper limit on the lifetime of the source.

From equation 11 the exponential can be expanded in a Taylor series

$$e^{(\underline{r}\cdot\underline{V}'\tau/\rho)^2/2r_0^2} \simeq 1 + \frac{(\underline{r}\cdot V'\tau/\rho)^2}{2r_0^2\ 1!} + \frac{(\underline{r}\cdot V'\tau/\rho)^4}{4r_0^4\ 2!} + \ldots \qquad (26)$$

to give the correlation function in terms of a series of integrals.

The n^{th} order contribution in $(V'\tau)^2$ is denoted by

$$R_n(\underline{p}_1,\underline{p}_2) = \frac{1}{(2\pi)^{3/2}r_0^2\rho} \int d^3r\ r^{2n}\ e^{-r^2/2r_0^2} \left[\frac{\underline{r}\cdot V'\tau}{\sqrt{2}\ r_0\rho}\right]^{2n} \frac{1}{n!}$$

$$\times \tfrac{1}{4}\{|{}^0\Psi(\underline{r},\Delta\underline{p})|^2 + \tfrac{3}{4}|{}^1\Psi(\underline{r},\Delta\underline{p})|^2\} \qquad (27)$$

The wave functions for relative motion are given by equation 15 in Section 3.2.1. The next step is the evaluation of the scalar product in the above equation. The relative position vector, $\underline{r}$, is defined in a coordinate frame with $\Delta\underline{p}$ along the z axis. The velocity vector $\underline{V}'$ is defined in a frame with the source velocity, $\underline{V}_0$ along the z axis. The transformation which rotates the laboratory frame into the CM frame is used to calculate the components of $\underline{V}'$ and the product $\underline{r}\cdot\underline{V}'$ may then be calculated. This product results in a series of terms involving powers of $\sin\theta$, $\cos\theta$, $\sin\phi$ and $\cos\phi$; θ and ϕ being the polar and azimuthal angles of $\underline{r}$ in the CM frame. The ϕ integration is done by hand, the orthogonality of $\cos\phi$ and $\sin\phi$ eliminating all terms involving odd powers of either.

The remaining integrations are carried out numerically using the programme CORFUN10. This programme first evaluates the τ=0 contribution to the correlation function and then calculates each successive order in $V'\tau$.

It calculates the integrals involving powers of $\cos\theta$ and Legendre polynomials using the recurrence relation

$$(L+1)P_{L+1}(x) - (2L+1)xP_{L}(x) + LP_{L-1}(x)=0$$

The results for each value of L are stored in an array. The sum over partial waves is then carried out, multiplying each term by the appropriate θ-integral, finally the sum over the orders of $V'\tau$ is performed and the radial integration performed

by calling a numerical integration routine.

The programme only calculates the first 10 orders, as the difficulty in calculating the ϕ-integral by hand limits the number of orders to be used. In fact, the convergence of the series for $V'_{r>r_0}$ is very poor. The next section describes a method for avoiding the series expansion which is valid for all r.

3.2.3 Alternative Derivation of The pp Correlation Function

Consideration of equation 11 will show that the integral cannot be calculated in terms of simple functions. The scalar product in the exponential effectively gives a "Gaussian-like" integral in the angular coordinates which can only be evaluated numerically. To avoid this difficulty an alternative approach is to change the form of the distribution function to a δ-function in space and keep the Gaussian in time. For collisions involving appreciable lifetimes this should not be too unphysical. It will, of course, only give an upper bound on the lifetime as any finite source size will reduce the correlation function. This arises because separating the particles in space or time both have the effect of reducing the correlation due to the short-range nuclear force.

We take then the form of the distribution function to be

$$D(\underline{r},t,\underline{p}) = \frac{1}{\sigma}\frac{d\sigma}{d\underline{p}}\frac{1}{\sqrt{\pi}\tau}\,\delta(\underline{r} - \underline{V}_0 t)e^{-t^2/\tau^2} \tag{28}$$

The normalisation condition is the same as for the Gaussian distribution function. Substituting equation 28 into equation 9 and following the procedure outlined in Appendix A to evaluate the correlation function gives the result

$$1 + R(\underline{p}_1,\underline{p}_2) = \frac{4}{(2\pi)^{1/2}V'\tau}\int_0^\infty dr\, e^{-r^2/2(V'\tau)^2}$$

$$\times \{P_s \Big| \sum_{L\ \text{even}} \Phi_L(kr)\, P_L(\cos\theta')\Big|^2$$

$$+ P_t \Big| \sum_{L\ \text{odd}} \Phi_L(kr)\, P_L(\cos\theta')\Big|^2\} \tag{29}$$

where θ' is the angle between $\underline{V}'$ and $\underline{V}_0$. We see that there is no angular dependence in equation 29 except that due to θ'. The assumption of a point source eliminates any dependence on the direction of $\Delta\underline{p}$. The source does however have a preferred direction given by the vector $\underline{V}'$ formed of the source velocity $\underline{V}_0$ and the pp CM velocity $\underline{V}$.

The numerical evaluation of equation 29 is straightforward. The same potential is used as in the previous section to generate the nuclear wave functions. In Figures 6a-c the two-proton correlation function obtained from the δ-function source is plotted against the relative momentum of the two

protons for several values of $V'\tau$. The data are taken from Reference 23 as before. The scattering angle is the angle between the beam velocity, $\underline{V}_0$, and the pp CM velocity, $\underline{V}$; it was set at 15° in these experiments. An upper limit on the source lifetime may be obtained from these graphs. For the Au data this limit is $V'\tau$ =18 fm and for the Al and C data $V'\tau$=30 fm. For 100 MeV protons this corresponds to a source lifetime in the range τ=16 - 27 x 10^{-23} sec. We shall discuss these results in Chapter 4.

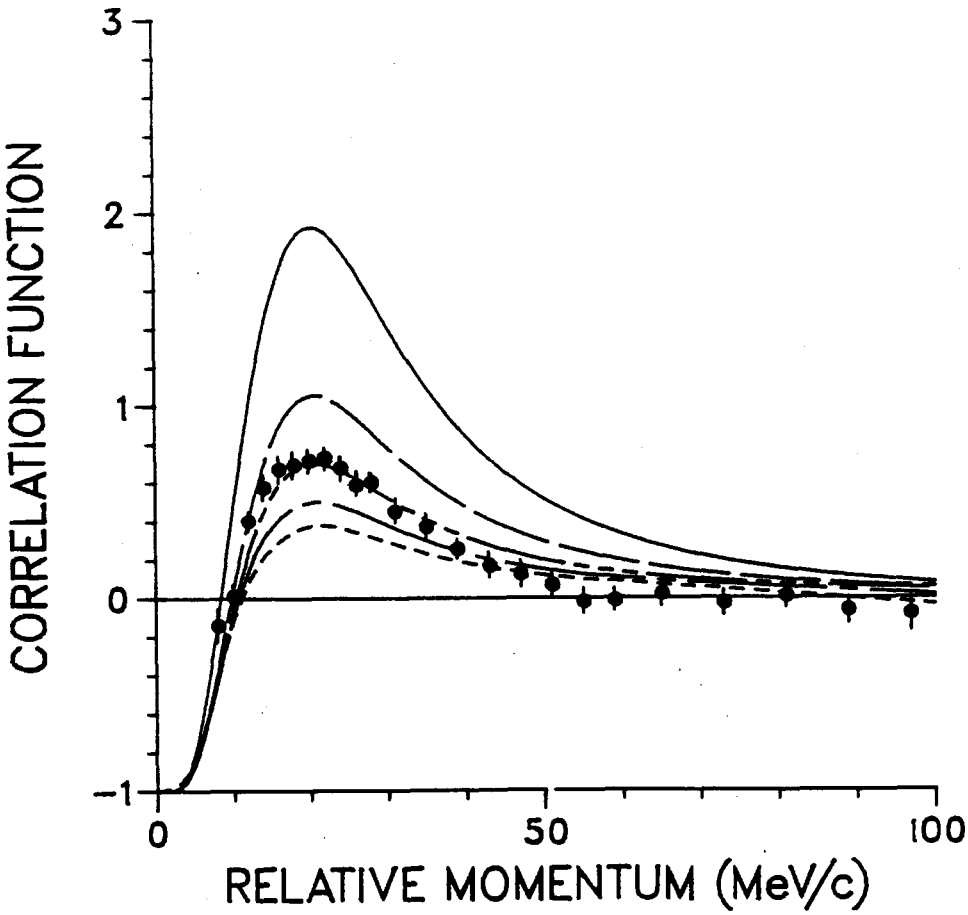

Figure 6a. Two-proton correlation function, $R(\underline{P}_1,\underline{P}_2)$, for a source with a δ-function shape in space and Gaussian time dependence. V' is the difference between the pp CM velocity and the source velocity, and τ is the source lifetime. Data are as Figure 5a for a gold target. The curve labels are:
V'τ=6 fm ————————, V'τ=12 fm———— ———— ,
V'τ=18 fm———— - - - —, V'τ=24 fm———— - ————,
V'τ=30 fm - - - - - - .

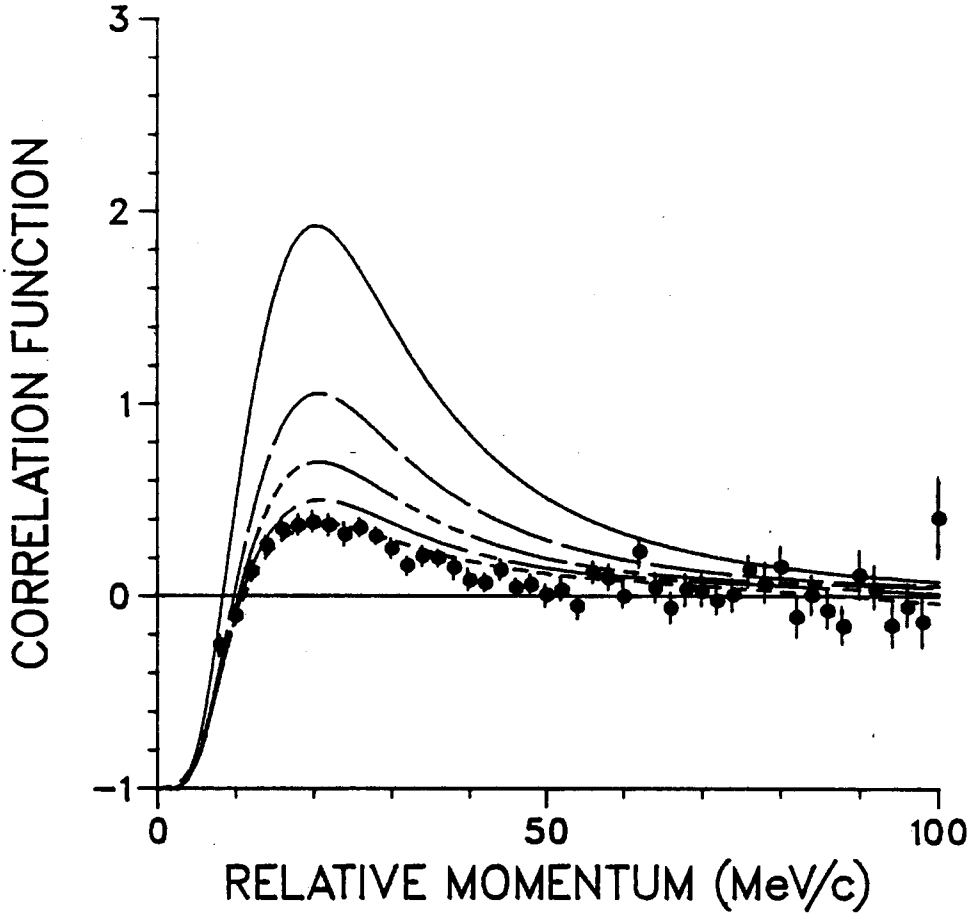

Figure 6b. Two-proton correlation function, $R(\underline{P}_1,\underline{P}_2)$, for a source with a δ-function shape in space and Gaussian time dependence. V' is the difference between the pp CM velocity and the source velocity, and τ is the source lifetime. Data are as Figure 5b for an aluminum target. The curve labels are:
V'τ=6 fm ————————, V'τ=12 fm———— ———— ,
V'τ=18 fm———— - - - - —, V'τ=24 fm———— - ————,
V'τ=30 fm- - - - - - -.

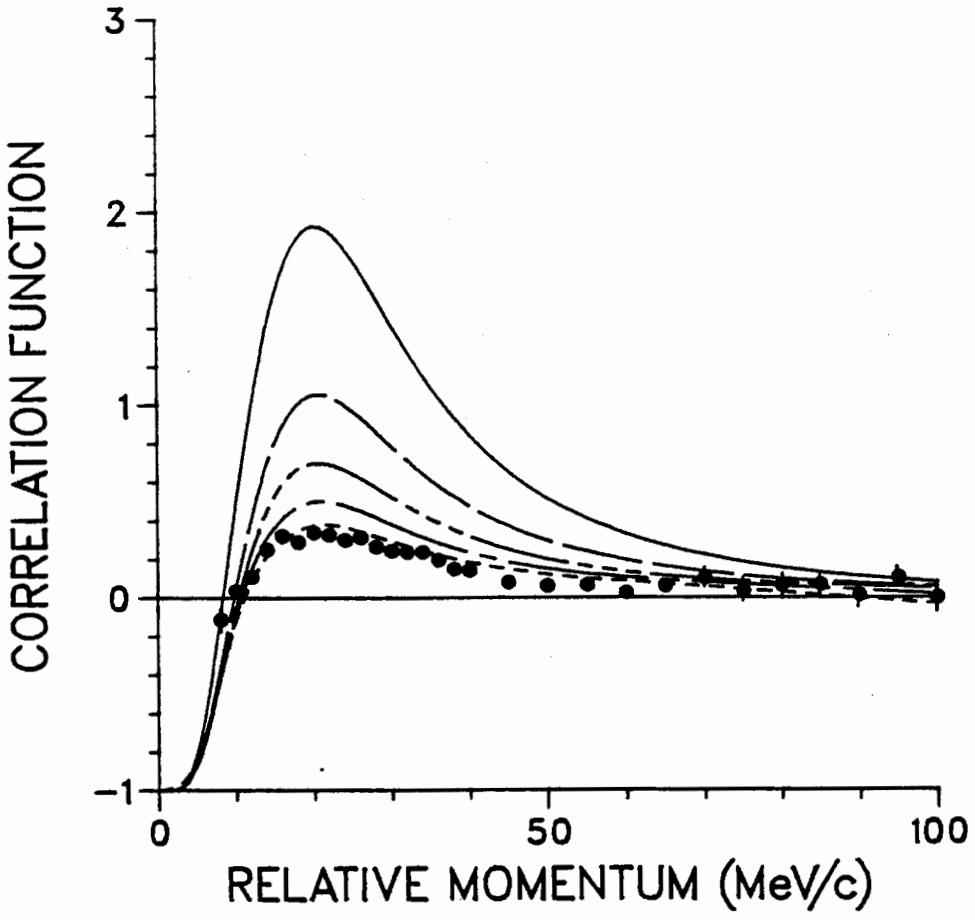

Figure 6c. Two-proton correlation function, $R(\underline{P}_1,\underline{P}_2)$, for a source with a δ-function shape in space and Gaussian time dependence. V' is the difference between the pp CM velocity and the source velocity, and τ is the source lifetime. Data are as Figure 5c for a carbon target. The curve labels are:
V'τ=6 fm ——————, V'τ=12 fm —— ——,
V'τ=18 fm — — — —, V'τ=24 fm —— - ——,
V'τ=30 fm - - - - - - -.

3.3 Extension to Deuterons and Tritons

3.3.1 Two-Deuteron Correlation Function

We see from the derivation of the pp correlation function that the fermion nature of the particles only appears in the wave functions. Hence to extend the correlation function to deuterons and other particles we need only to calculate their respective probability distributions, given by the square of the wave function for relative motion of the two particles. Since deuterons have spin 1, they may combine to form states of total spin 0, 1 or 2, with statistical weights 1/9, 3/9, 5/9 respectively. Because of the difficulties involved with the integral for non-zero lifetimes we choose the simpler case $\tau = 0$ in all that follows. As we shall see the correlation betweeen the particles drops rapidly as the particles become heavier and also we do not expect to be able to determine τ accurately from experiment. The two deuteron correlation function is then, by analogy with equation 12,

$$1 + R(\underline{p}_1,\underline{p}_2) = \frac{1}{(2\pi)^{3/2} r_0^3} \int d^3r \; e^{-r^2/2r_0^2} \times \{\tfrac{1}{9}|{}^0\Psi|^2 + \tfrac{3}{9}|{}^1\Psi|^2 + \tfrac{5}{9}|{}^2\Psi|^2\} \qquad (30)$$

The total spin of the two particles is labelled by a superscript. The evaluation of equation 30 is straightforward

and follows the same procedure as for the pp case.

The total wave function for relative motion of two deuterons must be symmetric under interchange of the two particles, and it may be shown, by examining the symmetry properties of the Clebsch-Gordan coefficients for combining two spin 1 particles, that even spin states are symmetric, odd spin states anti-symmetric. Hence the spin 0 and 2 wave functions in equation 30 consist of a sum over even L partial waves only, and the spin 1 wave function consists of odd L partial waves only. In this case, after doing the θ and ϕ integrals the equation becomes

$$1 + R(\underline{p}_1,\underline{p}_2) = \frac{2}{(2\pi)^{1/2}\, r_0^3} \int_0^\infty r^2 e^{-r^2/2r_0^2}\, dr$$

$$\times \left[\tfrac{1}{9}\left\{ \Sigma_{L \text{ even}} \left|{}^0\Phi_L\right|^2 \frac{2}{2L+1}\right\} + \tfrac{3}{9}\left\{ \Sigma_{L \text{ odd}} \left|{}^1\Phi_L\right|^2 \frac{2}{2L+1}\right\} + \tfrac{5}{9}\left\{ \Sigma_{L \text{ even}} \left|{}^2\Phi_L\right|^2 \frac{2}{2L+1}\right\}\right] \tag{31}$$

We have kept the superscript denoting the spin because the nuclear potential is spin dependent. We again evaluate equation 31 numerically. The nuclear potential is used in all partial waves with $L \leq 2$. Further, a given S and L may combine to form states with total angular momentum $J = S+L, S+L-1, \ldots, |S-L|$, and each state has $2J+1$ possible Z components of total angular momentum. The potential used is the Saxon-Woods form given in equation 32

$$V(\underline{r}) = \frac{V}{1+\exp((r-R)/a)} \qquad (32)$$

Two sets of potential parameters were used to generate the dd nuclear wave functions and are listed in Tables 1 and 2. The first set show a mainly repulsive potential and were obtained from the R matrix method of generating the dd phase shifts. [23] The second set are mainly attractive and come from the resonating group method[24].

TABLE 1

Saxon-Woods Potential Parameters For Repulsive dd Potential

S	L	J	V (MeV)	R (fm)	a (fm)
0	0	0	29.8	4.21	0.134
0	2	2	33.63	4.14	0.75
1	1	0	37.95	7.16	0.385
1	1	1	29.43	1.37	1.67
1	1	2	6.92	1.09	1.57
2	0	2	25.96	1.08	1.25
2	2	0	55.43	5.87	0.74
2	2	1	41.26	6.33	0.65
2	2	2	-11.53	1.85	1.69
2	2	3		–	
2	2	4		–	

TABLE 2

Saxon-Woods Potential Parameters For Attractive dd Potential

S	L	V (MeV)	R(fm)	a (fm)
0	0	-10.26	5.85	0.99
1	1	-13.83	3.64	0.87
2	0	-8.45	5.29	0.56
2	2	-15.24	2.56	1.08

The repulsive nuclear potential depends on S, L, J as given in Table 1. A statistical weight of $(2J+1)/(2S+1)(2L+1)$ was assigned to each J state to ensure the correct probability of occupation. Only the Coulomb potential was used in the highest S=2 states, as the nuclear phase shifts for these states were negligible. The attractive nuclear potential had no J dependence so only the spin statistical weight was used.

The Coulomb potential alone was used for all partial waves with L>2. The two potentials produce very different results for the correlation function. This can be seen from Figure 7 which shows the two-deuteron correlation function obtained with the repulsive and attractive nuclear potentials respectively. For comparison, the correlation function using the Coulomb potential only is also shown.

The attractive potential produces a result very similar to the pp correlation function, with a peak at $\Delta p \simeq 35$ MeV/c, whilst the repulsive potential suppresses the correlation function strongly. Figures 8a,b show the dd correlation function obtained with the repulsive nuclear potential, and data from the reaction $^{197}Au(^{16}O,dd)X$ and $^{12}C(^{16}O,dd)X$ from M.S.U.[23] It is clear that the data are well described by the phase shifts corresponding to the repulsive potential rather than the phase shifts obtained from the Resonating Group method, which produces the attractive potential. The source size obtained from the figures is r_0=6-8 fm which is larger than the corresponding proton case.

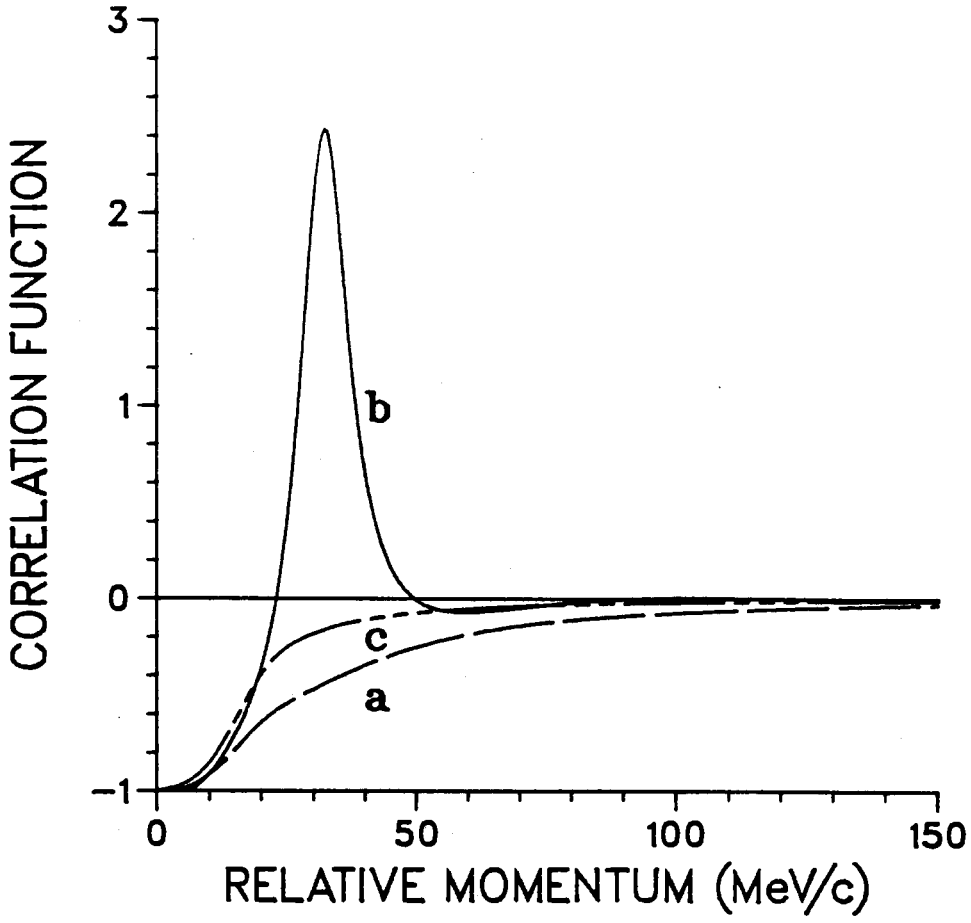

Figure 7. Two-deuteron correlation function, $R(\underline{P}_1,\underline{P}_2)$, for a source with a Gaussian shape in space and negligible lifetime assuming various dd potentials. The source radius is fixed at 6 fm. The curve labels are:

a). Repulsive nuclear plus Coulomb potential.
b). Attractive nuclear plus Coulomb potential.
c). Coulomb potential only.

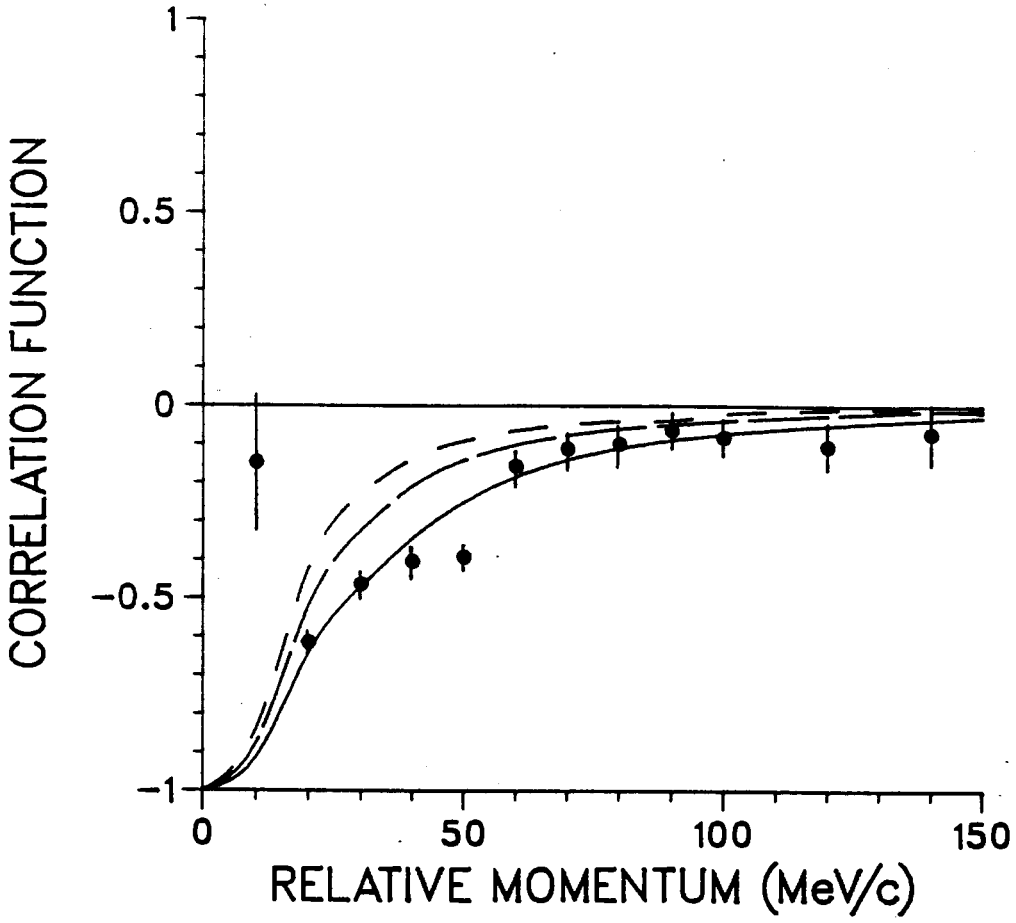

Figure 8a. Two-deuteron correlation function, $R(\underline{P}_1,\underline{P}_2)$, using the repulsive dd potential for a Gaussian source of negligible lifetime. Data as Figure 5a for a gold target. The curve labels are: r_o=6 fm ————, r_o=8 fm —— ——, r_o=10 fm— — —.

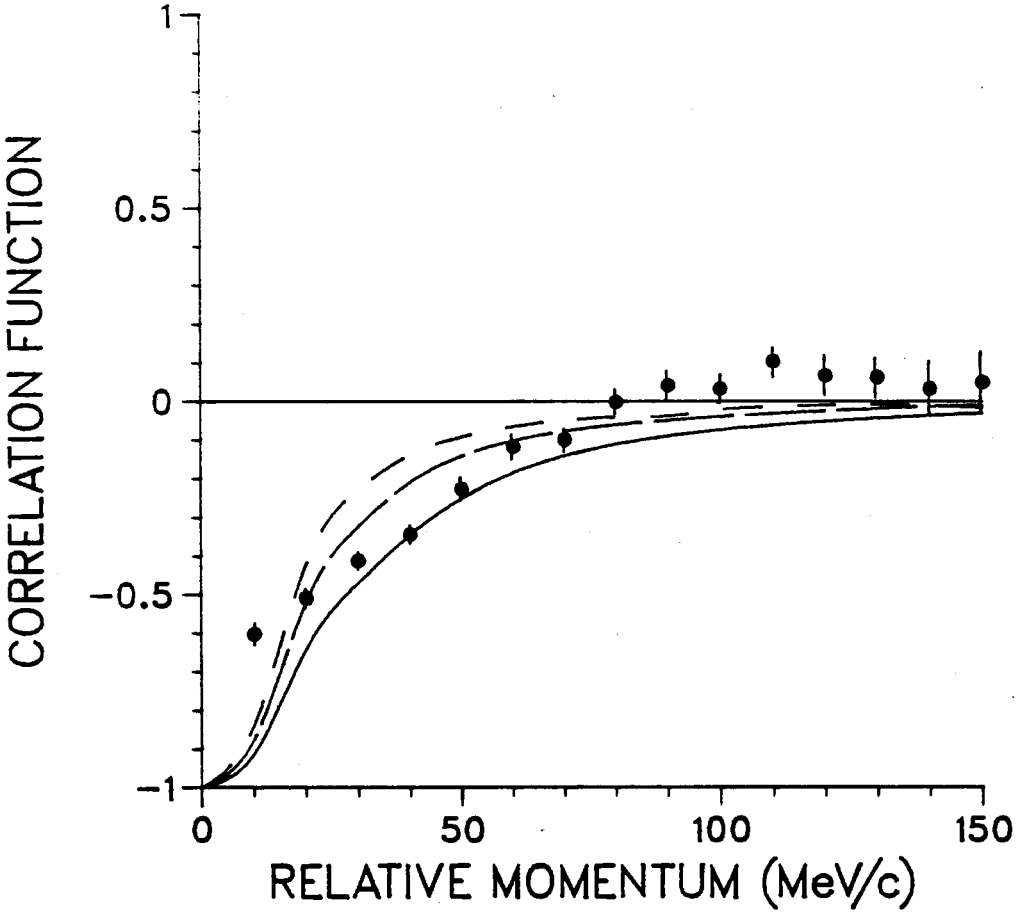

Figure 8b. Two-deuteron correlation function, $R(\underline{P}_1,\underline{P}_2)$, using the repulsive dd potential for a Gaussian source of negligible lifetime. Data as Figure 5c for a carbon target. The curve labels are: r_0=6 fm ————————, r_0=8 fm —— ——, r_0=10 fm— — —.

We conclude this section by looking at the dd correlation function in the absence of interactions except the effect of the Bose-Einstein statistics. In equation 30 the wave-functions are now just plane waves, with the S=0,2 waves being symmetric and the S=1 wave anti-symmetric under interchange of the two particles. Since now the S=0,2 waves are identical they may be combined to give

$$1 + R(\underline{p}_1,\underline{p}_2) = \frac{1}{(2\pi)^{3/2} r_0^3} \int d^3r\, e^{-r^2/2r_0^2} \times \{\tfrac{2}{3}|\Psi^s|^2 + \tfrac{1}{3}|\Psi^{as}|^2\} \qquad (33)$$

where $\Psi^s = \frac{1}{\sqrt{2}} \{ e^{i\underline{k}\cdot\underline{r}} + e^{-i\underline{k}\cdot\underline{r}} \} = \sqrt{2}\cos(\underline{k}\cdot\underline{r})$

$$\Psi^{as} = \frac{1}{\sqrt{2}} \{ e^{i\underline{k}\cdot\underline{r}} - e^{-i\underline{k}\cdot\underline{r}} \} = \sqrt{2}\, i \sin(\underline{k}\cdot\underline{r})$$

Putting these into equation 33 and evaluating the integral gives

$$R(\underline{p}_1,\underline{p}_2) = + \frac{1}{3} e^{-2k^2 r_0^2} \qquad (34)$$

This result differs from the simple derivation of C_2 only by the numerical factor of 1/3. For bosons there is thus an enhanced probability of finding two particles with equal final momenta, the 1/3 arising from the spin statistics for the

particles. Taking the limit as k goes to 0 gives R=+1/3, setting the potentials equal to zero in the programme again reproduced this limit.

By analogy with the proton case the Coulomb repulsion of the two protons in the deuterons causes a complete anti-correlation as the relative momentum goes to zero, hence the correlation function R goes to -1 in this limit.

3.3.2 Two-Triton Correlation Function

Figures 9a and 9b show the tt correlation function obtained with the Coulomb potential only. The data are taken from the M.S.U. and O.R.N.L. work[23] on the reaction $^{197}Au(^{16}O,tt)X$ and $^{12}C(^{16}O, tt)X$. At the beginning of the last section we pointed out that the spin of the particles only affects the wave functions. As the triton has spin 1/2 we may take over the results in section 3.2 by merely changing the reduced mass of two protons to that of two tritons.

Because of the difficulty in obtaining accurate nuclear potential parameters for the tt interactions, only the Coulomb potential was used in calculating the tt correlation function.

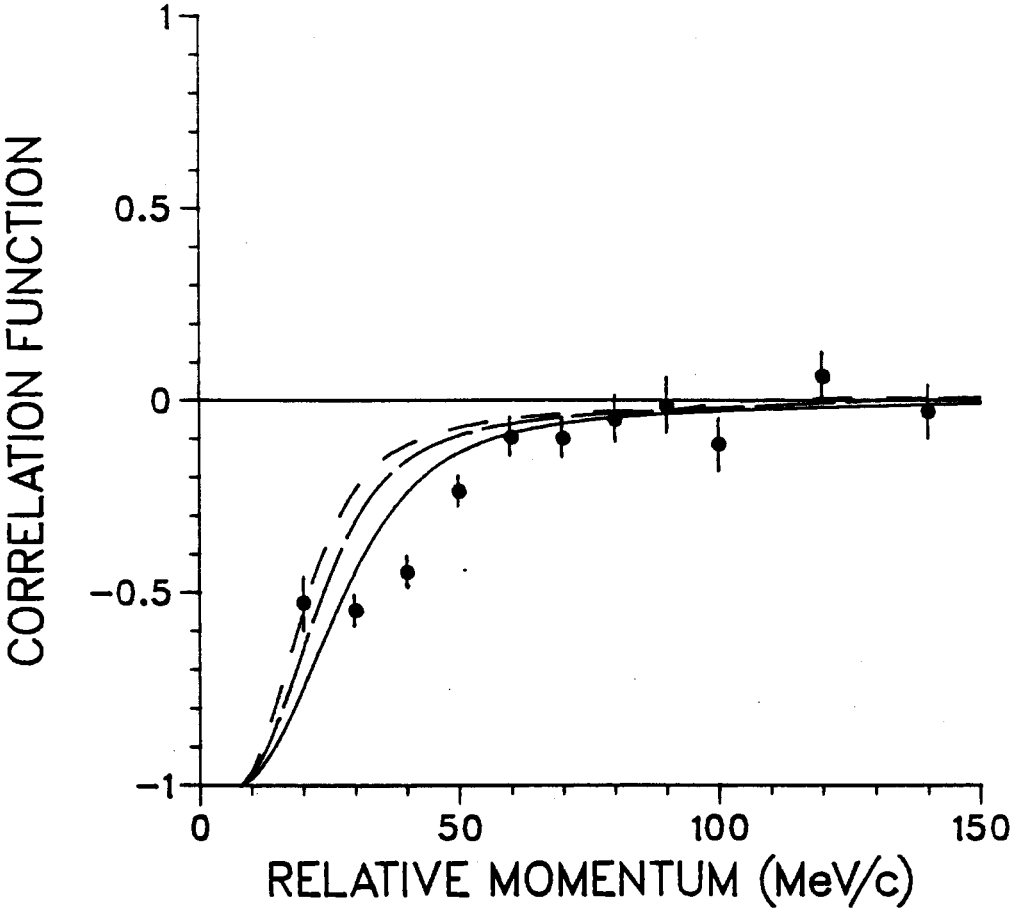

Figure 9a. Two-triton correlation function, $R(\underline{P}_1,\underline{P}_2)$, using the tt Coulomb potential only for a Gaussian source of negligible lifetime. Data as Figure 5a for a gold target. The curve labels are: r_0=6 fm ————, r_0=8 fm —— ——, r_0=10 fm — — —.

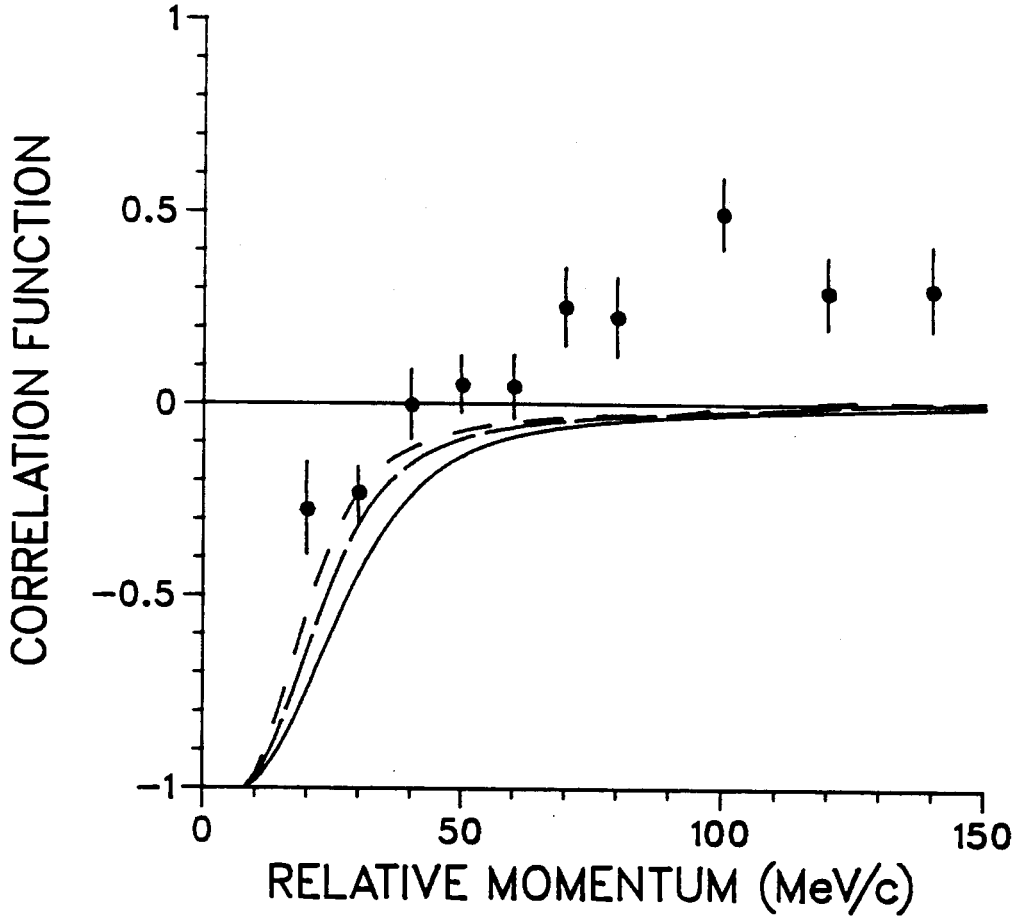

Figure 9b. Two-triton correlation function, $R(\underline{P}_1,\underline{P}_2)$, using the tt Coulomb potential only for a Gaussian source of negligible lifetime. Data as Figure 5c for a carbon target. The curve labels are: r_0=6 fm ————————, r_0=8 fm —— ——, r_0=10 fm — — —.

3.4 Discussion of Numerical Methods

The basic definition of the correlation function in Section 3 is in terms of an integral. Because this integral cannot be evaluated in terms of simple functions we must use a numerical integration routine. This introduces the first source of uncertainty into the result. Secondly, the partial wave expansion of the wave functions must be truncated at some value of the angular momentum. This will cause a drop in accuracy at large values of the relative momentum where more and more partial waves are important. Thirdly, the evaluation of the correlation function requires the values of Coulomb partial waves at arbitrary radial distances. To accomplish this the series expansion of the wave functions was used out to a certain maximum distance and the asymptotic form beyond that. The slight mismatching of the two sets of wave functions introduces another source of error.

The integrations were carried out using the Numerical Algorithms Group Routines D01GAF and D01AJF. The first of these returns the area under a set of points with an estimate of the error, the second integrates a given function to a specified relative accuracy and returns an estimate of the absolute error obtained. To minimize the errors from the routines the integrand was specified at 0.2 fm steps over the range 0-50 fm for the pp

calculations, and at 0.5 fm steps over the range 0-100 fm for the dd and tt calculations. The step size was 0.5 fm out to 150 fm for the calculation involving the δ-function distribution The relative accuracy for the second routine was specified at 10^{-6} for all cases except the non-zero τ calculation. To reduce the computer time needed for the calculation to manageable proportions it was set at 10^{-3}. In practice the estimate of the error returned by D01AJF was always negligible and that given by D01GAF was of the order of 5-10% for the non-zero τ case. The two routines were checked by integrating the exponential part of the integrand only and both returned almost exact answers.

The upper limit of the integration was set at $12R_0$, unless this exceeded 50 fm for the proton case, or 100 fm for the deuteron and triton cases. These distances were chosen as beyond them the exponential had rendered the integrand completely negligible. For the calculation using the δ-function source the integration was taken out to 150 fm for large values of $V'\tau$ to ensure the same drop in the exponential.

The error due to keeping only a finite number of partial waves in the expansion of the wave function is only important for relative momenta greater than 80 MeV/c. Because the correlation function is non-zero only in the range 0-70 MeV/c this source of error is negligible in this range. The calculation was done using 10 partial waves for the proton case and 15 for the deuteron and triton cases for $\Delta p \leq 80$ MeV/c which were increased to 15 and 24 partial waves respectively for $\Delta p > 80$

MeV/c.

The final source of error due to the change-over to asymptotic Coulomb waves at large values of kr is more important. The asymptotic form of the Coulomb waves is only strictly correct in the limit as kr goes to infinity. However by choosing the change-over point to be as large as possible (kr=15) the exponential had rendered the integrand negligible by the time the asymptotic waves were used, except for r_0=8-10 fm. For these values of r_0 it was still found to be negligible for relative momenta less than 60 MeV/c. Above this value the mismatch between the waves was of the order of 5-10%.

In summary the combined maximum probable error in the calculation amounts to 2-5% for relative momenta in the range 0-60 MeV/c and 5-10% for larger values.

4. Conclusions

4.1 Source Sizes from pp, dd and tt data (τ=0)

The conclusions from this work are divided into two sections: Firstly, we determine the 'Best-Fit' source sizes by comparison with the M.S.U./O.R.N.L. data from proton, deuteron and triton coincidence experiments, and secondly we examine the source lifetime dependence of the proton data. We discuss the implications of the results regarding the extent of final state interactions among the emitted particles and the degree of thermalisation achieved in HI reactions.

The Gaussian equivalent source sizes for negligible source lifetimes are obtained from Figures 5a-c,8a-b and 9a-b in Chapter 3. The results are shown in Table 3 below.

TABLE 3

Gaussian Equivalent Source Sizes

Reaction	Source Size (fm)
^{197}Au(^{16}O,pp)X	3.8±0.1
^{27}Al(^{16}O,pp)X	4.7±0.1
^{12}C(^{16}O,pp)X	4.9±0.1
^{197}Au(^{16}O,dd)X	6±1
^{12}C(^{16}O,dd)X	6±1
^{197}Au(^{16}O,tt)X	6±2

The results for the reaction $^{12}C(^{16}O,tt)X$ are not shown as the data do not allow an estimate of the source size to be made. This table shows that the protons are emitted from a region inside the collision volume about 3-4 fm in radius (actually this is the radius of the Gaussian corresponding to the source). This lends support to the fireball model which pictures the collision creating a small hot-spot inside the colliding nuclei which achieves thermal equilibrium and then decays by the random emission of particles.

This 'Lack of memory' of its history is characteristic of a system which is in a state of equilibrium. By contrast the direct model gives a strongly forward peaked differential cross-section where the particles retain some memory of the incident direction. We cannot however draw strong conclusions from this for two reasons: The calculation is effectively impact parameter averaged since we asssumed the existence of a distribution function for emission of a particle which had no dependence on the way the source was created, and, the single-particle inclusive data do not allow us to eliminate the direct model completely.

The size of the 'hot-spot' (3-4 fm) is smaller than the radius of the target nucleus ($\simeq$7 fm for gold target) and hence it appears that only a sub-set of the target nucleons attains thermal equilibrium. This result is important for estimating the extent of thermalisation in HI collisions in order to see if a possible hadron liquid-gas phase transition has any measureable

effects.

One surprising result of the data is that the source size seems to increase with decreasing target mass. This is best seen from the proton data where the radius is 3.8, 4.7, 4.9 fm for the Au, Al and C targets respectively. This result cannot depnd on the energy of the emitted particles as the experimental procedure used to generate the data involved summing over all energies and angles of emission corresponding to a given relative momentum. This corresponds to a significant averaging process as stated in Reference 11. Naively, one would expect a heavier target nucleus to reach thermal equilibrium more easily as the number of possible collisions (which transfer energy and momentum to the surrounding nucleons) increases with target mass. This would lead to a larger source size for a gold target than, say, a carbon one. A possible explanation of the result is that energy is lost in the light target collision in moving the CM of the system whereas the heavy target stays essentially at rest and all the kinetic energy of the incident beam is converted into thermal energy rapidly heating up the system which then emits particles sooner (with respect to the time of impact) than the lighter targets.

The results of the deuteron and triton experiments show that the source sizes are significantly larger (6-8 fm) than in the proton case (3-4 fm). This agrees with the picture of the source heating up to a temperature of,say,tens of MeV and emitting high energy protons whereas the low binding energy of

the deuteron and triton causes them to break up in these early stages of the reaction. Later in the collision, after the source has expanded and cooled down the emission of heavier bound particles takes place.

4.2 Source Lifetimes from Proton data

Figures 6a-c show the pp correlation function from the δ-function calculation for the Au, Al and C targets respectively. In this case the correlation function is a function only of $V'\tau$. The energy of the emitted particles enters the calculation through V' via the velocity of the pp centre of mass. Figure 10 shows the contours of r_0 and $V'\tau$ consistent with the peak in the correlation function data for detecting protons of a given kinetic energy. This data is also from M.S.U./O.R.N.L.[26] but involved only counting events corresponding to protons with energies in a given range.

The series solution gives an upper bound on the source lifetime of 8.6×10^{-23} sec for 50 MeV protons assuming a realistic Gaussian source radius of 2.4 fm. This time will decrease for higher energy protons. From figures 6a-c we see that the δ-function approach gives an upper limit of 16-40 x 10^{-23} sec for protons with energies in the range 50-100 MeV.

It can be seen from figure 10 that the accuracy of the calculation decreases as $V'\tau$ increases. For increasing values of $V'\tau$ more terms have to be kept in the series expansion in order

to achieve the same accuracy, as we have kept only 10 the error due to neglecting higher order terms becomes progressively larger. This error is less than the numerical errors involved if $V'\tau \leq r_0$, for larger values of $V'\tau$ the two sources of error are combined.

Thus we see that the source lifetime is at most of the order of 10-30 x 10^{-23} seconds, which is much less than that needed to form a compound nucleus (10^{-20} - 10^{-21} sec) which may be ruled out under these circumstances.

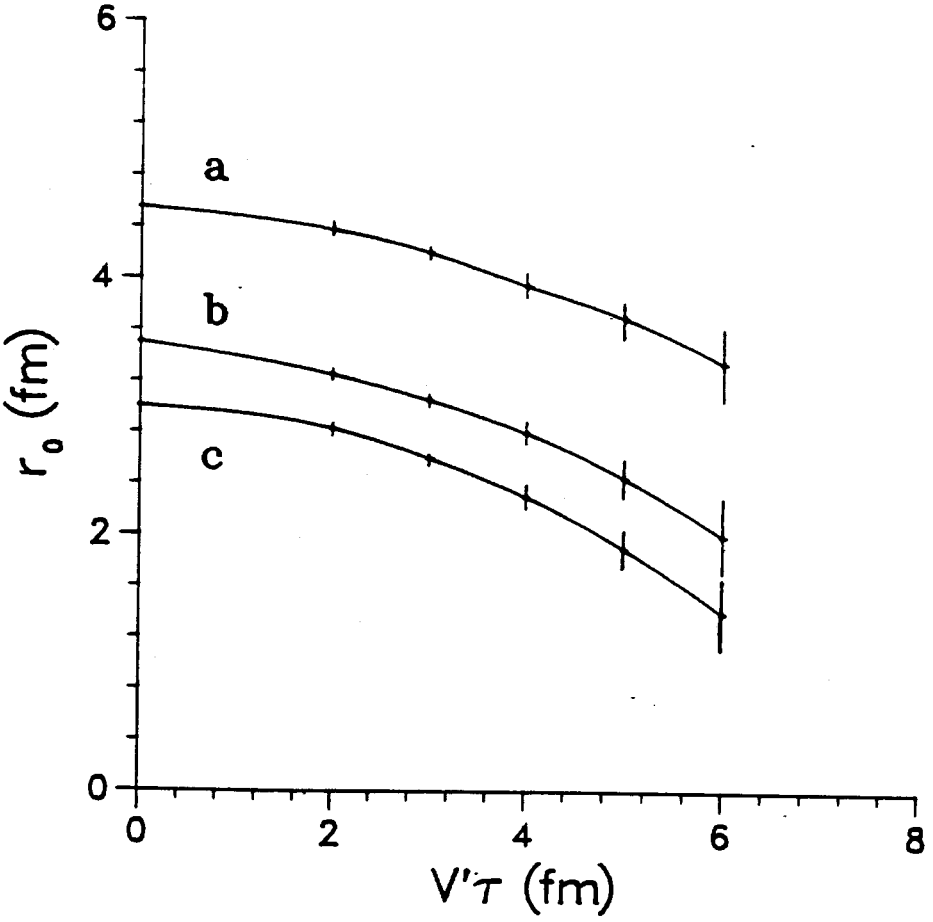

Figure 10. Contours of Gaussian equivalent source radii r_o and lifetime τ which produce a pp correlation function consistent with the data from Figure 2 of Ref. 26. The curves are for different ejectile energies:

a) E_1+E_2 = 60 MeV.
b) E_1+E_2 = 80 MeV.
c) E_1+E_2 = 100 MeV.

The final point to be made is the importance of final state interactions among the emitted particles. The simple calculation presented in section 1.2 neglected these interactions and produced the typical exponential decay seen in the stellar interferometry of Hanbury-Brown and Twiss. Also, data from pion interferometry are corrected for final state interactions by using a simple Gamow factor. In this work, however, it is obvious that final state interactions among the particles are very important. The large peak in the pp correlation function at small relative momenta and the suppression of the correlation function for all particles as the relative momentum goes to zero show that the particles interact via the strong nuclear and Coulomb forces for an appreciable time after the collision. Similarly, the deuteron data show that the dd potential is predominantly repulsive which implies that the phase shifts obtained from the resonating group method (which produce the large positive peak in the dd correlation function) must be rejected in favour of those produced by the R matrix method. Neglecting the nuclear interaction between tritons seems to be justified by the fairly good agreement between the curve produced with the Coulomb interaction only and the gold data.

Appendix A

1. Derivation of Two-Proton Correlation Function with a Gaussian Source

We start with the definitions given in Chapter 3. The two-proton correlation function is defined in terms of the two-particle coincidence cross-section by

$$\frac{1}{\sigma}\frac{d^2\sigma}{d\underline{p}_1 d\underline{p}_2} = \int dt_1\, dt_2\, d^3r_1\, d^3r_2\, D(\underline{r}_1,t_1,\underline{p})\, D(\underline{r}_2,t_2,\underline{p})$$

$$\times \left\{ \tfrac{1}{4} \left| {}^0\Psi_{\underline{p}_1\underline{p}_2}(\underline{r}_1',\underline{r}_2)\right|^2 + \tfrac{3}{4} \left| {}^1\Psi_{\underline{p}_1\underline{p}_2}(\underline{r}_1',\underline{r}_2)\right|^2 \right\} \qquad \text{(A1)}$$

The distribution function for a Gaussian source is

$$D(\underline{r},t,\underline{p}) = \frac{1}{\sigma}\frac{d\sigma}{d\underline{p}} \frac{1}{\pi^2 r_0^3 \tau} e^{-(\underline{r}-\underline{V}_0 t)^2/\underline{r}_0^2} e^{-t^2/\tau^2} \qquad \text{(A2)}$$

where r_0, τ are measures of the spatial and temporal extent of the source. The distribution function satisfies the normalisation condition

$$\int d^3r\, dt\, D(\underline{r},t,\underline{p}) = \frac{1}{\sigma}\frac{d\sigma}{d\underline{p}} \qquad \text{(A3)}$$

In A2, $(\underline{r}-\underline{V}_0 t)$ appears because we expect the source to move with a non-zero laboratory velocity, $\underline{V}_0$, taken to be along the beam direction. The definition A2 applies in the lab frame. For convenience we can write

$$C_2(\underline{p}_1,\underline{p}_2) = \left[\frac{1}{\sigma} \frac{d^2\sigma}{d\underline{p}_1 d\underline{p}_2} \right] / \left[\frac{1}{\sigma} \frac{d\sigma}{d\underline{p}} \right]^2 \qquad (A4)$$

The wave functions ${}^0\Psi$, ${}^1\Psi$ are the product of a plane wave in the CM coordinates $\underline{R} = (\underline{r}_1'+\underline{r}_2)/2$, and the wave function Ψ_{Rel} for relative motion which depends on the relative coordinates $\underline{r}'=\underline{r}_1'-\underline{r}_2$. Here $\underline{r}_1'=\underline{r}_1+\underline{V}(t_2-t_1)$ and represents the fact that at time t_2 the particle created at $(\underline{r}_1,t_1)$ has moved to $(\underline{r}_1',t_2)$. The velocity of the proton is $\underline{V} = \underline{P}/M$, where $\underline{P}$ is the total laboratory momentum of the protons and M is twice the proton mass. The CM wave function disappears on taking the modulus squared and so the wave function depends only on the relative momentum, $\Delta\underline{p}=(\underline{p}_1-\underline{p}_2)/2$ and relative position $\underline{r}'$. Again for convenience we write

$$\Phi(\underline{r}',\Delta\underline{p}) = \tfrac{1}{4}\left| {}^0\Psi_{\underline{p}_1\underline{p}_2}(\underline{r}_1',\underline{r}_2)\right|^2 + \tfrac{3}{4}\left| {}^1\Psi_{\underline{p}_1\underline{p}_2}(\underline{r}_1',\underline{r}_2)\right|^2 \qquad (A5)$$

With these definitions, A1 become

$$C_2(\underline{p}_1,\underline{p}_2) = \frac{1}{\pi^4 r_0^6 \tau^2}\int dt_1\, dt_2\, d^3r_1\, d^3r_2\, e^{-(t_1^2+t_2^2)/\tau^2}$$

$$\times\, e^{-(\underline{r}_1-\underline{V}_0 t_1)^2/r_0^2}\, e^{-(\underline{r}_2-\underline{V}_0 t_2)^2/r_0^2}\, \Phi(\underline{r}',\Delta\underline{p}) \qquad (A6)$$

Changing to CM and relative coordinates in space and time

$$\underline{R}=\{\underline{r}_1'+\underline{r}_2\}/2$$

$$\underline{r}'=\underline{r}_1'-\underline{r}_2$$

$$T=\{t_1+t_2\}/2$$

$$t=t_1-t_2 \qquad (A7)$$

and using $\underline{r}' = \underline{r}_1+\underline{V}(t_2-t_1)$ enables us to rewrite equation A6 in terms of the new variables. The 'volume' element transforms as

$$d^3r_1\, d^3r_2\, dt_1\, dt_2 = d^3R\, d^3r'\, dT\, dt$$

and so

$$C_2(\underline{p}_1,\underline{p}_2) = \frac{1}{\pi^4 r_0^6 \tau^2}\int dt_1\, dt_2\, d^3R\, d^3r'$$

$$\times\, e^{-\{\underline{R}+\frac{1}{2}\underline{r}'+\underline{V}t-\underline{V}_0(T+\frac{1}{2}t)\}^2/r_0^2}\, e^{-\{\underline{R}-\frac{1}{2}\underline{r}'-\underline{V}_0(T-\frac{1}{2}t)\}^2/r_0^2}$$

$$\times\, e^{-\{(T+\frac{1}{2}t)^2+(T-\frac{1}{2}t)^2\}/\tau^2}\, \Phi(\underline{r}',\Delta\underline{p})$$

doing the integrals over dT and d^3R gives

$$C_2(\underline{p}_1,\underline{p}_2) = \frac{1}{(2\pi)^2 r_0^3 \tau} \int dt\, d^3r'$$

$$\times e^{-\{\frac{1}{2}r'^2 + \underline{r}'\cdot\underline{V}'t + \frac{1}{2}(V't)^2\}/r_0^2} e^{-t^2/2\tau^2} \Phi(\underline{r}',\Delta\underline{p})$$

Finally, doing the dt integral gives

$$C_2(\underline{p}_1,\underline{p}_2) = \frac{1}{(2\pi)^{3/2} r_0^2 \rho} \int d^3r'$$

$$\times e^{-\{r'^2-(\underline{r}'\cdot\underline{V}'\tau/\rho)^2\}/2r_0^2} \Phi(\underline{r}',\Delta\underline{p}) \qquad \text{(A8)}$$

Where $\underline{V}'=\underline{V}-\underline{V}_0$, $\rho^2=r_0^2+(V'\tau)^2$ and the prime on $\underline{r}'$ may now be dropped as it is a dummy variable. Remembering that $C_2(\underline{p}_1,\underline{p}_2) = 1 + R(\underline{p}_1,\underline{p}_2)$ gives the desired result (Equation 11, Chapter 3)

2. Derivation of Two-Proton Correlation Function with a δ-Function Source

We follow the same procedure as in part 1 of this appendix, except that now the distribution function for emission of a proton is

$$D(\underline{r},t,\underline{p}) = \frac{1}{\sigma}\frac{d\sigma}{d\underline{p}}\frac{1}{\sqrt{\pi}\tau}\delta(\underline{r}-\underline{V}_0 t)e^{-t^2/\tau^2} \qquad \text{(A9)}$$

The δ-function is normalized by

$$\int d^3r\ \delta(\underline{r}-\underline{V}_0 t) = 1 \qquad \text{(A10)}$$

Thus A9 satisfies the normalisation condition A3. The analogue of equation A6 is

$$C_2(\underline{p}_1,\underline{p}_2) = \frac{1}{\pi\tau^2} \int d^3r_1\ d^3r_2\ dt_1\ dt_2\ \delta(\underline{r}_1-\underline{V}_0 t_1)\ \delta(\underline{r}_2-\underline{V}_0 t_2)$$
$$\times\ e^{-(t_1^2+t_2^2)/\tau^2}\ \Phi(\underline{r}',\Delta\underline{p}) \qquad \text{(A11)}$$

All terms being as defined before. Changing variables using the relations A7 and doing the d^3R and dT integrals gives

$$C_2(\underline{p}_1,\underline{p}_2) = \frac{1}{\sqrt{(2\pi)}\tau} \int d^3r'\ dt\ \delta(\underline{r}'+\underline{V}'t)\ e^{-t^2/2\tau^2}\ \Phi(\underline{r}',\Delta\underline{p})$$

To eliminate the second δ-function the two angular integrations and the t integration may be used. Firstly, we note that the t integral has the range $-\infty$ to $+\infty$ and so we split it into two parts; $-\infty$ to 0 and 0 to $+\infty$. Letting t go to -t in the first part then gives

$$C_2(\underline{p}_1,\underline{p}_2) = \frac{1}{\sqrt{(2\pi)}\tau} \int d^3r' \int_0^\infty dt\ \delta(\underline{r}'-\underline{V}'t)\ e^{-t^2/2\tau^2}\ \Phi(\underline{r}',\Delta\underline{p})$$
$$+ \frac{1}{\sqrt{(2\pi)}\tau} \int d^3r' \int_0^\infty dt\ \delta(\underline{r}'+\underline{V}'t)\ e^{-t^2/2\tau^2}\ \Phi(\underline{r}',\Delta\underline{p})$$

(A12)

Now we know

$$\delta(\underline{r}'-\underline{V}'t)= \frac{1}{|r'^2\sin\theta|}\ \delta(r-V't)\ \delta(\theta-\theta')\ \delta(\phi-\phi') \qquad (A13)$$

where (θ,ϕ) and (θ',ϕ') are the polar and azimuthal angles of $\underline{r}$ and $\underline{V}'$ respectively in the coordinate frame with $\underline{V}_o$ along the z axis. Also

$$\delta(\underline{r}+\underline{V}'t)= \frac{1}{|r'^2\sin\theta|}\ \delta(r-V't)\ \delta(\theta-\{\pi-\theta'\})\ \delta(\phi-\{\pi+\phi'\})$$

as $\underline{V}'=-(-\underline{V}')$ and letting $\underline{V}'\rightarrow-\underline{V}'$ is equivalent to letting $\theta' \rightarrow\pi-\theta'$, $\phi'\rightarrow\pi+\phi'$. From equation A5 the sign of V' makes no difference to the function $\Phi(\underline{r}',\Delta\underline{p})$. This being so, the two terms in A12 may be added, and using

$$\delta(r-V't)= \frac{1}{|V'|}\ \delta(t-r/V')$$

gives

$$C_2(\underline{p}_1,\underline{p}_2) = \frac{4}{\sqrt{(2\pi)}V'\tau}\int_0^\infty dr\ e^{-r^2/2(V'\tau)^2}$$

$$\times\ \{\ P_s\ |\ \sum_{L\ \text{even}}\Phi_L(kr)\ P_L(\cos\theta')|^2 + P_t\ |\ \sum_{L\ \text{odd}}\Phi_L(kr)\ P_L(\cos\theta')|^2\} \qquad (A14)$$

which is what we wanted to show (Equation 29, Chapter 3).

Appendix B

```
C       PROGRAMME SCHROPP NUMERICALLY INTEGRATES
C       SCHRODINGER'S EQUATION.
        IMPLICIT REAL*8 (A-H,O-Y)
        INTEGER S,L
        LOGICAL FLAG
        DIMENSION PSI(50001),RSTO(50001)
        DO 5 I=1,50001
        RSTO(I)=0.D0
5       PSI(I)=0.D0
C
C       INPUT STEP LENTGH
C
        DELR=0.01D0
        KMAX=10001
        RSTO(1)=0.D0
        RSTO(2)=DELR
        PSI(1)=0.D0
        PSI(2)=0.01D0
        L=0
C
C       REID SOFT-CORE L=0 POTENTIAL PARAMETERS.
C
C       NB. HARDCORE RADIUS OF RC .LT. 0.01 FM MUST BE INCLUDED.
C       (I.E. RSTO(2) MUST BE GREATER THAN 0.01 FM)
C
        V1=-14.947D0
        A1=0.7D0
        V2=-2358.D0
        A2=2.8D0
        V3=9263.14D0
        A3=4.9D0
C
C       LOOP OVER MOMENTA
C
C       DO 300 IK=1,3
        IK=1
        FLAG=.TRUE.
        R=DELR
        H2OM=41.5D0
        HBC=197.33D0
        P=DFLOAT(20*IK)
        AK=P/HBC
        F1=DFLOAT(2*L+1)
        F2=DFLOAT(L*(L+1))
        E=P**2/938.258D0
```

```
      AMA=0.D0
      DO 100 K=3,50001
C     WRITE(6,75)R,RSTO(K)
75    FORMAT(1X,2G10.5)
      R=R+DELR
      RSTO(K)=R
      IF((R*A3).LT.150.D0) GO TO 95
C     IF(FLAG) WRITE(6,86)R
86    FORMAT(1X,'ERROR R TOO LARGE FOR EXPONENT',D15.5)
      FLAG=.FALSE.
      V=0.D0
      GO TO 96
C
C     REID SOFT-CORE POTENTIAL.
C
95    V=(V1/DEXP(A1*R)+V2/DEXP(A2*R)+V3/DEXP(A3*R))/R
C
96    DER=(V+(1.44D0/R)+(F2*H2OM/R**2)-E)/H2OM
      KM1=K-1
      KM2=K-2
      PSI(K)=2.D0*PSI(KM1)-PSI(KM2)+DER*(DELR**2)*PSI(KM1)
90    IF(RSTO(K).LT.100.D0)GO TO 100
      TEST=DABS(PSI(K))
C     WRITE(6,55)RSTO(K),PSI(K),AMA
55    FORMAT(1X,F10.5,2G15.6)
      IF(TEST.GT.AMA)AMA=TEST
100   CONTINUE
C
C     END OF CALCULATION
C
C     WRITE(6,200)AMA
200   FORMAT(1X,'AMA=',G15.6)
C
C     OUTPUT WAVE FUNCTIONS
C
      WRITE(6,110)AK
110   FORMAT(1X,D15.8)
      DO 150 K=1,KMAX,20
      IF(RSTO(K).LE.0.1D0)GO TO 145
      PSI(K)=F1*PSI(K)/(AMA*AK*RSTO(K))
145   WRITE(6,120)RSTO(K),PSI(K)
120   FORMAT(1X,F8.2,2X,D15.8)
121   FORMAT(1X,D15.8)
150   CONTINUE
300   CONTINUE
      STOP
      END
```

```
C
C
C       PROGRAMME TO CALCULATE THE PP CORRELATION FUNCTION IN
C       HEAVY-ION COLLISIONS ASSUMING A GAUSSIAN DISTRIBUTION
C       FUNCTION FOR EMISSION OF A PROTON.
C
C
C       J.C.SHILLCOCK  S.F.U. AUGUST 1984.
C
C
        IMPLICIT REAL*8 (A-H,O-Y)
        REAL*8 W(1600),X(251),Y(251),YR0(251),YT(251)
        REAL*8 K,MOD
        REAL*8 PI/3.14159265359D0/,C/2.9979246D+08/
        COMPLEX*16 SUM
        INTEGER LMAX,LMIN,NMAX,IW(202)
        LOGICAL FLAG
        EXTERNAL INTGND,INTGN
        COMMON /AREA/ B,K,RO,LMAX,LMIN,NMAX
        COMMON /ARRAY/ P(31,31,31),F(10,21)
        COMMON /BOX/ GAM3,PS,PT /BOX2/ EPSILN,RMAX
C
C       INPUT PARAMETERS AND INITIALISE CONSTANTS.
C       READ UNIT 2=INPUTFILE
C
C       DELTA P = PP RELATIVE MOMENTUM VECTOR
C       RO      = RADIUS OF SOURCE (FM)
C       TAU     = LIFETIME OF SOURCE (SEC)
C       VO      = LAB.SOURCE VELOCITY (UNITS OF C)
C       V       = PP LAB. VELOCITY (UNITS OF C)
C       VPRIME  = V-VO (UNITS OF C)
C       THETA   = POLAR ANGLE BETWEEN V AND VO (DEGREES)
C       PHI     = AZIMUTHAL          "
C       THETAV  = POLAR ANGLE BETWEEN VPRIME AND VO (DEGREES)
C       ALPHA   = POLAR ANGLE BETWEEN DELTA P AND VO (DEGREES)
C       BETA    = AZIMUTHAL          "
C
        CALL TIME(0)
        FLAG=.FALSE.
C
        READ(2,43)NR,NE
43      FORMAT(I2,1X,I2)
C
C       NR    =  NO. OF RUNS TO BE MADE
C       NE    =  NO. OF VALUES OF RELATIVE MOMENTA TO BE USED
C       NW    =  NO. OF VALUES OF NUCLEAR WAVE FUNCTIONS READ IN
C                (ARRAYS CONTAINING NUCLEAR WAVE FUNCTIONS MUST
C                HAVE AT LEAST DIMENSION NW)
C       RW    =  UPPER LIMIT TO INTEGRATION (FM.)
C       RMAX  =  "DISTANCE"AT WHICH ASYMPTOTIC WAVE FUNCTIONS ARE
C                USED
C       LMIN  =  MIN. COULOMB ONLY PARTIAL WAVE
C       LMAX  =  MAX.   "     "     "       "   (ARRAY P MUST HAVE
```

```
C                DIMENSION AT LEAST 2*LMAX+1)
C      NMAX   =  NO. OF ORDERS (ARRAY F MUST HAVE DIMENSION AT
C                LEAST 2*NMAX+1)
C      PS/PT  =  STATISTICAL WEIGHTS OF EVEN/ODD L STATES
C
C      FUNCTIONS7:NW=251 RW=50.(STEP 0.01)
C
       NW=251
       RMAX=15.D0
       PS=0.25D0
       PT=0.75D0
C
C      LOOP FOR DIFFERENT PARAMETER VALUES.
C
       DO 1500 INR=1,NR
C
       READ(2,20)RO,VO,V,TAU,THETA,PHI,ALPHA,BETA
20     FORMAT(3D10.6,E10.6,4D6.2)
       WRITE(6,15)
15     FORMAT(1X,3HP-P,2X,17HPARAMETER VALUES:)
C
C      SET UPPER LIMIT OF INTEGRATION = 12*RO
C      AND RESET CONSTANTS FOR NEXT RUN.
C
       NMAX=10
       LMIN=1
       LMAX=10
       RW=12.D0*RO
       IF(RW.GT.50.D0)RW=50.D0
       THETA=(THETA*PI)/180.D0
       PHI=(PHI*PI)/180.D0
       ALPHA=(ALPHA*PI)/180.D0
       BETA=(BETA*PI)/180.D0
       VX=V*DSIN(THETA)*DCOS(PHI)
       VY=V*DSIN(THETA)*DSIN(PHI)
       VZ=V*DCOS(THETA)
       VPRIME=DSQRT(V**2+VO**2-2.D0*V*VO*DCOS(THETA))
       VPRIMZ=VZ-VO
       THETAV=DARCOS(VPRIMZ/VPRIME)
       GAM3=DSIN(ALPHA)*DSIN(THETAV)*(DCOS(BETA)*DCOS(PHI)+
      #DSIN(BETA)*DSIN(PHI))+DCOS(ALPHA)*DCOS(THETAV)
       IF(TAU.EQ.0.D0) GO TO 30
       VTAU=VPRIME*TAU*C*1.D+15
       RHO=DSQRT(RO**2+VTAU**2)
       EPSILN=(VTAU/(RO*RHO))**2/2.D0
       GO TO 40
30     RHO=RO
       VTAU=0.D0
       EPSILN=0.D0
       GO TO 42
C
40     IF(FLAG)GO TO 32
C
```

```
C      EVALUATION OF INTEGRALS OF LEGENDRE POLYNOMIALS
C      AND POWERS OF COS(THETA).
C
         DO 70 I=1,31
         DO 70 J=1,31
         DO 70 JK=1,31
         P(I,J,JK)=0.D0
70       CONTINUE
C
C      SET UP N=0 INTEGRALS FOR L=1,30
C
       P(1,1,1)=2.D0
       NM2=2*NMAX
         DO 80 L=1,30
         P(L+1,L+1,1)=2.D0/DFLOAT(2*L+1)
80       CONTINUE
C
C      SET UP N>0 INTEGRALS FOR L=1,2*LMAX
C
         DO 90 I=1,NM2
         DO 90 L=1,30
         DO 90 M=1,30
         P(L+1,M+1,I+1)=(DFLOAT(L+1)*P(L+2,M+1,I)+
      #  DFLOAT(L)*P(L,M+1,I))/DFLOAT(2*L+1)
         P(1,M+1,I+1)=P(2,M+1,I)
         IF(I.GT.NMAX)GO TO 90
         P(1,1,2*I+1)=2.D0/DFLOAT(2*I+1)
90       CONTINUE
C
C        CALCULATE LEGENDRE POLYNOMIALS ONLY ONCE
C
         FLAG=.TRUE.
32       CONTINUE
C
C      ANGULAR FUNCTIONS ARISING FROM PHI INTEGRATION
C
         DO 35 IB=1,10
         DO 35 IC=1,21
         F(IB,IC)=0.D0
35       CONTINUE
       G=GAM3
       GP=1.D0-G*G
       G2=G*G
       G4=G2*G2
       G6=G4*G2
       G8=G6*G2
       G10=G8*G2
       G12=G10*G2
       G14=G12*G2
       G16=G14*G2
       G18=G16*G2
       G20=G18*G2
       F(1,1)=GP
```

```
 F(1,3)=3.D0*G2-1.D0
 F(2,1)=0.75D0*GP*GP
 F(2,3)=1.5D0*GP*(5.D0*G2-1.D0)
 F(2,5)=0.75D0*GP*(1.D0-9.D0*G2)+2.D0*G4
 F(3,1)=0.625D0*(GP**3)
 F(3,3)=1.875D0*GP*GP*(7.D0*G2-1.D0)
 F(3,5)=1.875D0*GP*(GP*(1.D0-13.D0*G2)+8.D0*G4)
 F(3,7)=0.625D0*GP*(GP*(19.D0*G2-1.D0)-24.D0*G4)+2.D0*G6
 F(4,1)=0.546875D0*(GP**4)
 F(4,3)=2.1875D0*(GP**3)*(9.D0*G2-1.D0)
 F(4,5)=3.28125D0*GP*GP*(GP*(1.D0-17.D0*G2)+16.D0*G4)
 F(4,7)=0.4375D0*GP*(5.D0*GP*(GP*(25.D0*G2-1.D0)-48.D0
#*G4)+64.D0*G6)
 F(4,9)=0.109375D0*GP*(5.D0*GP*(GP*(1.D0-33.D0*G2)
#+96.D0*G4)-256.D0*G6)+2.D0*G8
 F(5,1)=0.4921875D0*(GP**5)
 F(5,3)=2.4609375D0*(GP**4)*(11.D0*G2-1.D0)
 F(5,5)=1.640625D0*(GP**3)*(3.D0*GP*(1.D0-21.D0*G2)+
#80.D0*G4)
 F(5,7)=4.921875D0*GP*GP*(GP*(GP*(31.D0*G2-1.D0)-80.D0*G4)+
#32.D0*G6)
 F(5,9)=0.3515625D0*GP*(7.D0*GP*(GP*(GP*(1.D0-41.D0*G2)+
#160.D0*G4)-128.D0*G6)+128.D0*G8)
 F(5,11)=0.0078125*GP*(7.D0*GP*(3.D0*GP*(3.D0*GP*
#(51.D0*G2-1.D0)-800.D0*G4)+2880.D0*G6)-5760.D0*G8)+
#+2.D0*G10
 F(6,1)=0.451171875D0*(GP**6)
 F(6,3)=2.70703125D0*(GP**5)*(13.D0*G2-1.D0)
 F(6,5)=6.767578125D0*(GP**4)*(GP*(1.D0-25.D0*G2)+
#40.D0*G4)
 F(6,7)=9.0234375D0*(GP**3)*(GP*(GP*
#(37.D0*G2-1.D0)-120.D0*G4)+64.D0*G6)
 F(6,9)=0.966796875D0*GP*GP*(7.D0*GP*(GP*(GP*(1.D0-49.D0
#*G2)+240.D0*G4)-256.D0*G6)+384.D0*G8)
 F(6,11)=0.12890625D0*GP*(3.D0*GP*(7.D0*GP*(GP*(GP*
#(61.D0*G2-1.D0)-400.D0*G4)+640.D0*G6)-1920.D0*G8)+
#512.D0*G10)
 F(6,13)=0.064453125D0*GP*(GP*(7.D0*GP*(GP*(GP*
#(1.D0-73.D0*G2)+600.D0*G4)-1280.D0*G6)+5760.D0*G8)
#-1024.D0*G10)+2.D0*G12
 F(7,1)=0.4189453125D0*(GP**7)
 F(7,3)=2.9326171875D0*(GP**6)*(15.D0*G2-1.D0)
 F(7,5)=8.7978515625D0*(GP**5)*(GP*(1.D0-29.D0*G2)
#+56.D0*G4)
 F(7,7)=14.6630859375D0*(GP**4)*(GP*(GP*(43.D0*G2-1.D0)
#-168.D0*G4)+112.D0*G6)
 F(7,9)=14.6630859375D0*(GP**3)*(GP*(GP*(GP*(1.D0-57.D0*G2)
#+336.D0*G4)-448.D0*G6)+128.D0*G8)
 F(7,11)=2.9326171875D0*(GP**2)*(3.D0*GP*(GP*(GP*(GP*
#(71.D0*G2-1.D0)-560.D0*G4)+1120.D0*G6)-640.D0*G8)
#+256.D0*G10)
 F(7,13)=0.088867D0*GP*(33.D0*GP*(GP*(GP*(GP*(GP*(1.D0
#-85.D0*G2)+840.D0*G4)-2240.D0*G6)+1920.D0*G8)
```

```
#-512.D0*G10)+1024.D0*G12)
 F(7,15)=0.0126953125D0*GP*(33.D0*GP*(GP*(GP*(GP*(GP*
#(99.D0*G2-1.D0)-1176.D0*G4)+3920.D0*G6)-4480.D0*G8)
#+1792.D0*G10)-7168.D0*G12)+2.D0*G14
 F(8,1)=0.39276123D0*(GP**8)
 F(8,3)=-3.14208984D0*(GP**8)+50.2734375D0*(GP**7)*G2
 F(8,5)=10.99731445*(GP**8)-351.9140625D0*(GP**7)*G2+
#821.1328125D0*(GP**6)*G4
 F(8,7)=-21.9946289D0*(GP**8)+1055.7421875D0*(GP**7)*G2
#-4926.796875D0*(GP**6)*G4+3941.4375D0*(GP**5)*G6
 F(8,9)=27.49328613D0*(GP**8)-1759.570313D0*(GP**7)*G2+
#12316.99219D0*(GP**6)*G4-19707.1875D0*(GP**5)*G6+
#7038.28125D0*(GP**4)*G8
 F(8,11)=-21.99462891D0*(GP**8)+1759.570313D0*
#(GP**7)*G2-16422.65625D0*(GP**6)*G4+39414.375D0*
#(GP**5)*G6-28153.125D0*(GP**4)*G8+
#5005.D0*(GP**3)*G10
 F(8,13)=10.99731445D0*(GP**8)-1055.742188D0*(GP**7)*G2+
#12316.99219D0*(GP**6)*G4-39414.375D0*(GP**5)*G6+
#42229.6875D0*(GP**4)*G8-15015.D0*(GP**3)*G10+
#1365.D0*(GP**2)*G12
 F(8,15)=-3.14208984D0*(GP**8)+351.9140625D0*(GP**7)*G2
#-4926.796875D0*(GP**6)*G4+19707.1875D0*(GP**5)*G6
#-28153.125D0*(GP**4)*G8+15015.D0*(GP**3)*G10
#-2730.D0*(GP**2)*G12+120.D0*GP*G14
 F(8,17)=0.39276123D0*(GP**8)-50.2734375D0*(GP**7)*G2+
#821.1328125D0*(GP**6)*G4-3941.4375D0*(GP**5)*G6+
#7038.28125D0*(GP**4)*G8-5005.D0*(GP**3)*G10+
#1365.D0*(GP**2)*G12-120.D0*GP*G14+2.D0*G16
 F(9,1)=0.370941D0*(GP**9)
 F(9,3)=-3.33847D0*(GP**9)+60.092468D0*(GP**8)*G2
 F(9,5)=13.35388D0*(GP**9)-480.73975D0*(GP**8)*G2+
#1281.972656D0*(GP**7)*G4
 F(9,7)=-31.159058D0*(GP**9)+1682.589D0*(GP**8)*G2
#-8973.80859D0*(GP**7)*G4+8375.555D0*(GP**6)*G6
 F(9,9)=46.73859D0*(GP**9)-3365.1782D0*(GP**8)*G2+
#26921.426D0*(GP**7)*G4-50253.328D0*(GP**6)*G6+
#21537.14D0*(GP**5)*G8
 F(9,11)=-46.73859D0*(GP**9)+4206.4728D0*(GP**8)*G2
#-44869.043D0*(GP**7)*G4+125633.32D0*(GP**6)*G6
#-107685.7D0*(GP**5)*G8+23930.156D0*(GP**4)*G10
 F(9,13)=31.159D0*(GP**9)-3365.178D0*(GP**8)*G2+
#44869.043D0*(GP**7)*G4-167511.1D0*(GP**6)*G6+
#215371.4D0*(GP**5)*G8-95720.625D0*(GP**4)*G10+
#11602.5D0*(GP**3)*G12
 F(9,15)=-13.35388D0*(GP**9)+1682.589D0*(GP**8)*G2
#-26921.4D0*(GP**7)*G4+125633.3D0*(GP**6)*G6-215371.4D0*
#(GP**5)*G8+143580.9D0*(GP**4)*G10-34807.5D0*
#(GP**3)*G12+2295.D0*GP*GP*G14
 F(9,17)=3.33847D0*(GP**9)-480.73975D0*(GP**8)*G2+
#8973.8D0*(GP**7)*G4-50253.33D0*(GP**6)*G6+107685.7D0*
#(GP**5)*G8-95720.625D0*(GP**4)*G10+34807.5D0*(GP**3)
#*G12-4590.D0*GP*GP*G14+153.D0*GP*G16
```

```
      F(9,19)=-0.370941D0*(GP**9)+60.092D0*(GP**8)*G2-1281.97D0*
     #(GP**7)*G4+8375.55D0*(GP**6)*G6-21537.1D0*(GP**5)*G8+
     #23930.156D0*(GP**4)*G10-11602.5D0*(GP**3)*G12+2295.D0*
     #GP*GP*G14-153.D0*GP*G16+2.D0*G18
      F(10,1)=0.352394D0*(GP**10)
      F(10,3)=-3.52394D0*(GP**10)+17.6198D0*(GP**9)*G2
      F(10,5)=15.857735D0*(GP**10)-158.57735D0*(GP**9)*G2+
     #1902.928D0*(GP**8)*G4
      F(10,7)=-42.2873D0*(GP**10)+634.3094D0*(GP**9)*G2
     #-15223.425D0*(GP**8)*G4+16238.32D0*(GP**7)*G6
      F(10,9)=74.0028D0*(GP**10)-1480.05D0*(GP**9)*G2+53282.D0*
     #(GP**8)*G4-113668.2D0*(GP**7)*G6+56834.1D0*(GP**6)*G8
      F(10,11)=-88.8033D0*(GP**10)+2220.08D0*(GP**9)*G2
     #-106564.D0*(GP**8)*G4+341004.7D0*(GP**7)*G6
     #-341004.7D0*(GP**6)*G8+90934.6D0*(GP**5)*G10
      F(10,13)=74.0028D0*(GP**10)-2220.083D0*(GP**9)*G2+
     #133205.D0*(GP**8)*G4-568341.2D0*(GP**7)*G6+
     #852511.8D0*(GP**6)*G8-454673.D0*(GP**5)*G10+
     #68889.8D0*(GP**4)*G12
      F(10,15)=-42.28729D0*(GP**10)+1480.055D0*
     #(GP**9)*G2-106564.D0*(GP**8)*G4+568341.2D0*(GP**7)*G6
     #-1136682.4D0*(GP**6)*G8+909345.9D0*(GP**5)*G10
     #-275559.4D0*(GP**4)*G12+24225.D0*(GP**3)*G14
      F(10,17)=15.857735D0*(GP**10)-634.094D0*(GP**9)*G2+
     #53282.D0*(GP**8)*G4-341004.7D0*(GP**7)*G6+852511.8D0*
     #(GP**6)*G8-909345.9D0*(GP**5)*G10+413339.1D0*(GP**4)
     #*G12-72675.D0*(GP**3)*G14+3583.75D0*GP*GP*G16
      F(10,19)=-3.523941D0*(GP**10)+158.57735D0*(GP**9)*G2
     #-15223.425D0*(GP**8)*G4+113668.24D0*(GP**7)*G6
     #-341004.7D0*(GP**6)*G8+454673.D0*(GP**5)*G10
     #-275559.375D0*(GP**4)*G12+72675.D0*(GP**3)*G14
     #-7167.5D0*GP*GP*G16+190.D0*GP*G18
      F(10,21)=0.352394D0*(GP**10)-17.6197D0*(GP**9)*G2+
     #1902.928D0*(GP**8)*G4-16238.32D0*(GP**7)*G6+56834.12D0*
     #(GP**6)*G8-90934.59D0*(GP**5)*G10+68889.8D0*(GP**4)*G12
     #-24225.D0*(GP**3)*G14+3583.75D0*GP*GP*G16-190.D0*GP*G18
     #+2.D0*G20
C
C     LIST VARIABLES
C
42    WRITE(6,45)VO,V,VPRIME,VTAU,TAU,THETA,PHI,RO,RHO,EPSILN
45    FORMAT(1H1,5X,'VO    =',F15.6/6X,'V     =',F15.6/6X,
     #'VPRIME=',F15.6/6X,'VTAU  =',F15.6/6X,
     #'TAU   =',E15.6/6X,'THETA =',F15.6/6X,'PHI   =',F15.6/6X,
     #'RO    =',F15.6/6X,'RHO   =',F15.6/
     #6X,'EPSILN=',F15.6)
      WRITE(6,46)THETAV,ALPHA,BETA
46    FORMAT(6X,'THETAV=',F15.6/6X,'ALPHA =',F15.6/6X,'BETA  =',
     #F15.6//)
C     WRITE(6,39)
39    FORMAT(1X,'READING IN WAVE-FUNCTIONS')
C
C
```

```
C      INPUT NUCLEAR WAVE FUNCTIONS FROM FILE:READ UNIT 5
C      TAU=0,ZEROTH ORDER CONTRIBUTION TO R
C
C
55     DO 1000 IK=1,NE
       ANS=0.D0
       ER=0.D0
       IF(LMIN.NE.0)GO TO 58
       K=DFLOAT(5*IK)/197.33D0
       GO TO 101
58     READ(5,60)K
60     FORMAT(1X,D15.8)
       IF(K.GE.0.4D0)LMAX=12
C
         DO 100 IR=1,NW
         X(IR)=0.D0
         Y(IR)=0.D0
         YR0(IR)=0.D0
         READ(5,75)X(IR),YR0(IR)
75       FORMAT(1X,F8.2,2X,D15.8)
         IF(X(IR).GT.RW) GO TO 100
         Y(IR)=2.D0*PS*(YR0(IR)**2)
      #  *(X(IR)**2)/DEXP(0.5D0*(X(IR)/RO)**2)
100      CONTINUE
       CALL D01GAF(X,Y,NW,ANS,ER,IFAIL)
101    B=0.0173491215D0/K
       CALL D01AJF(INTGND,0.D0,RW,0.D0,1.D-06,RESULT,ABSERR,W,
      #1600,IW,202,IFAIL)
       ANSWR=2.D0*(ANS+RESULT)/(DSQRT(2.D0*PI)*RO*RO*RHO)
       ERROR=2.D0*(ER+ABSERR)/(DSQRT(2.D0*PI)*RO*RO*RHO)
       IF(TAU.EQ.0.D0) GO TO 2000
C
C
C      TAU>0,Nth ORDER CONTRIBUTION TO R
C
C
C
C
       ANS=0.D0
       RESULT=0.D0
C
C      WRITE(6,103)
103    FORMAT(1X,'STARTING LOOP OVER ORDER')
C
       IF(LMIN.EQ.0)GO TO 140
         DO 130 IR=1,NW
         Y(IR)=0.D0
         IF(X(IR).GT.RW) GO TO 130
104      NFACT=1
           DO 120 N=1,NMAX
           NFACT=NFACT*N
           NM3=2*N+2
           NM4=NM3-1
```

```
          YT(IR)=0.D0
            DO 110 IM=1,NM4
            M=IM-1
            DO 110 II=2,NM3,2
            I=II-2
            IF(P(1,M+1,I+1).EQ.0.D0) GO TO 110
            IF(M.NE.0)GO TO 105
            YT(IR)=YT(IR)+F(N,I+1)*P(1,1,I+1)*(YR0(IR)**2)
            GO TO 110
C
C     TEST TO SEE IF ASYMPTOTIC COULOMB WAVES ARE NECESSARY
C
105         IF(X(IR).GT.(RMAX/K))GO TO 107
            CALL COULO(X(IR),M,SUM,MOD)
            GO TO 108
107         CALL COULA(X(IR),M,SUM,MOD)
108         YT(IR)=YT(IR)+2.D0*F(N,I+1)*P(1,M+1,I+1)*YR0(IR)
     #       *MOD*DREAL(SUM)
110         CONTINUE
          Y(IR)=Y(IR)+YT(IR)*(X(IR)**NM3)*(EPSILN**N)/
     #           DFLOAT(NFACT)
120       CONTINUE
        Y(IR)=PS*Y(IR)/DEXP(0.5D0*(X(IR)/RO)**2)
130     CONTINUE
C     WRITE(6,133)
133   FORMAT(1X,'CALLING D01GAF'/)
      CALL D01GAF(X,Y,NW,ANS,ER,IFAIL)
C
C    COULOMB PARTIAL WAVE CONTRIBUTION TO R
C

140   CALL D01AJF(INTGN,0.D0,RW,0.D0,1.D-03,RESULT,ABSERR,W,
     #1600,IW,202,IFAIL)
      ANSWR=ANSWR+(ANS+RESULT)/(DSQRT(2.D0*PI)*RO*RO*RHO)
      ERROR=ERROR+(ER+ABSERR)/(DSQRT(2.D0*PI)*RO*RO*RHO)
2000  ANSWR=ANSWR-1.D0
      P2=197.33D0*K
      WRITE(6,1200)P2,ANSWR,ERROR
1200  FORMAT(1X,'P=',F10.5,5X,'R=',D18.8,2X,D18.8)
1000  CONTINUE
C
      REWIND 5
1500  CONTINUE
      CALL TIME(1,-1,ITIME)
C
      STOP
      END
C
C
C     SUBROUTINE INTGND RETURNS THE VALUE OF THE INTEGRAND
C     FOR NAG ROUTINE D01AJF AT EACH POSITION R,FOR TAU=0.
C     IT USES COULC TO CALCULATE EACH COULOMB PARTIAL WAVE.
C
```

```
C
      REAL FUNCTION INTGND*8 (R)
      IMPLICIT REAL*8 (A-H,O-Y)
      REAL*8 MOD
      COMPLEX*16 SUM,CMOD
      COMMON /AREA/ A,D,E,L1,L2,NMAX
      COMMON /BOX/ T,PS,PT /BOX2/ EPSILN,RMAX
      INTGND=0.D0
      IF(R.GT.(12.D0*E))RETURN
      AMOD1=0.D0
      AMOD2=0.D0
      L3=L2+1
      L4=L1+1
C
C     PARTIAL WAVE LOOP
C
        DO 100 IL=L3,L4
        L=IL-1
        IT=(-1)**(L+1)
C
C       TEST TO SEE IF ASYMPTOTIC COULOMB WAVES ARE NECESSARY.
C
C       NB. COULC AND COULCA RETURN THE PRODUCT OF PARTIAL WAVES
C       DIFFERING BY "DELTA" UNITS.IF DELTA=0,THEY RETURN THE
C       MODULUS SQUARED OF THE Lth WAVE.
C
        IF(R.GT.(RMAX/D))GO TO 50
        CALL COULC(R,L,0,SUM,CMOD)
        GO TO 55
50      CALL COULCA(R,L,0,SUM,CMOD)
C
C     PARTIAL WAVE SUM; AMOD1 = EVEN L WAVES
C                       AMOD2 = ODD  L WAVES
C
55      IF(IT)60,70,80
60      AMOD1=AMOD1+2.D0*CMOD*SUM/DFLOAT(2*L+1)
        GO TO 70
80      AMOD2=AMOD2+2.D0*CMOD*SUM/DFLOAT(2*L+1)
70      CONTINUE
100     CONTINUE
C
C     RETURN VALUE OF INTGND
C
      INTGND=R*R*(PS*AMOD1+PT*AMOD2)/DEXP(0.5D0*(R/E)**2)
      RETURN
      END
C
C
C     SUBROUTINE COULC RETURNS THE PRODUCT OF PARTIAL WAVES
C     DIFFERING BY "DELTA" UNITS.
C
C
      SUBROUTINE COULC(R,L,DELTA,SUM,CMOD)
```

```
      IMPLICIT REAL*8 (A-H,O-Y)
      INTEGER DELTA,L1,L2,NMAX
      REAL*8 MOD,MOD1,PI/3.14159265359D0/
      COMPLEX*16 CMOD,AN,AND,SUM,SUMD,Z
      COMMON /AREA/ A,D,E,L1,L2,NMAX
      F=D*R
      MOD=1.D0
      IF(A.NE.0.D0)MOD=2.D0*A*PI/(DEXP(2.D0*A*PI)-1.D0)
      CMOD=DCMPLX(DCOS(DFLOAT(DELTA)*PI/2.D0),DSIN(DFLOAT(DELTA)
     #*PI/2.D0))
C
C     CALCULATE PRODUCT OF HYPERGEOMETRIC FUNCTIONS
C     AND THE MAGNITUDE OF THE COULOMB WAVE.
C
      Z=DCMPLX(0.D0,-2.D0*F)
      AN=DCMPLX(1.D0,0.D0)
      SUM=DCMPLX(0.D0,0.D0)
      AND=DCMPLX(1.D0,0.D0)
      SUMD=DCMPLX(0.D0,0.D0)
C
        DO 40 IN=1,101
C
        IF(IN.LE.L)MOD=MOD*F*F*(1.D0+(A*A)/DFLOAT(IN*IN))/
     #  DFLOAT((2*IN-1)**2)
        IF(IN.GT.DELTA) GO TO 30
        MOD=MOD*2.D0*F/DFLOAT((2*(L+IN))*(2*(L+IN)-1))
        CMOD=CMOD*DCMPLX(DFLOAT(L+IN),A)
C
30      N=IN-1
        SUM=SUM+AN
        SUMD=SUMD+AND
        AN=AN*Z*DCMPLX(DFLOAT(L+1+N),A)/DFLOAT((2*L+2+N)*(1+N))
        AND=AND*Z*DCMPLX(DFLOAT(L+DELTA+1+N),A)/DFLOAT
     #  ((2*(L+DELTA)+2+N)*(1+N))
40      CONTINUE
      SUM=DCONJG(SUM)*SUMD
      CMOD=DCMPLX(MOD,0.D0)*CMOD
      RETURN
      END
C
C
C     SUBROUTINE COULO RETURNS THE VALUE OF THE Lth PARTIAL WAVE
C     REQUIRED BY NAG ROUTINE D01GAF TO CALCULATE THE
C     CONTRIBUTION FROM COUPLING BETWEEN  WAVES.
C
C
      SUBROUTINE COULO(R,L,SUM,MOD)
      IMPLICIT REAL*8 (A-H,O-Y)
      REAL*8 MOD,PI/3.14159265359D0/
      COMPLEX*16 AN,SUM,Z
      COMMON /AREA/ A,D,E,L1,L2,NMAX
      F=D*R
      MOD=1.D0
```

```
      IF(A.NE.0.D0)MOD=DSQRT(2.D0*A*PI/(DEXP(2.D0*A*PI)-1.D0))
      ARG1=-0.5772156649D0
      ARG2=0.D0
      Z=DCMPLX(0.D0,-2.D0*F)
      AN=DCMPLX(1.D0,0.D0)
      SUM=DCMPLX(0.D0,0.D0)
        DO 40 IN=1,101
        IF(IN.GT.L) GO TO 20
        MOD=MOD*F*DSQRT(1.D0+(A*A)/DFLOAT(IN*IN))/DFLOAT(2*IN-1)
        ARG1=ARG1+1.D0/DFLOAT(IN)
20      ARG2=ARG2+A/DFLOAT(L+IN)-DATAN(A/DFLOAT(L+IN))
        N=IN-1
        SUM=SUM+AN
        AN=AN*Z*DCMPLX(DFLOAT(L+1+N),A)/DFLOAT((2*L+2+N)*(1+N))
40      CONTINUE
      ARG=A*ARG1+ARG2
      SUM=SUM*DCMPLX(DCOS(F+ARG+DFLOAT(L)*PI/2.D0),DSIN(F+ARG+
     #DFLOAT(L)*PI/2.D0))
      RETURN
      END
C
C
C     FUNCTION INTGN RETURNS THE VALUE OF THE Nth ORDER
C     INTEGRAND REQUIRED BY D01AJF.
C
C
      REAL FUNCTION INTGN*8 (R)
      IMPLICIT REAL*8 (A-H,O-Y)
      COMPLEX*16 SUM,CMOD
      INTEGER DELTA
      COMMON /AREA/ A,D,E,L1,L2,NMAX
      COMMON /ARRAY/ P(31,31,31),F(10,21)
      COMMON /BOX/ T,PS,PT /BOX2/ EPSILN,RMAX
      INTGN=0.D0
      IF(R.GT.(15.D0*E))RETURN
      NFACT=1
      DO 130 N=1,NMAX
      NFACT=NFACT*N
      N2=2*N+2
      N3=N2-1
      AMOD1=0.D0
      AMOD2=0.D0
      IF(L2.NE.0)GO TO 60
C
C     L=0 COULOMB PARTIAL WAVE
C
        AMODT=0.D0
        DO 50 IM=1,N3
        M=IM-1
C
        IF(R.GT.(RMAX/D))GO TO 20
        CALL COULC(R,0,M,SUM,CMOD)
        GO TO 30
```

```
20        CALL COULCA(R,0,M,SUM,CMOD)
30        DO 50 II=2,N2,2
          I=II-2
          IF(P(1,M+1,I+1).EQ.0.D0)GO TO 50
          AMODT=AMODT+F(N,I+1)*P(1,M+1,I+1)*DREAL(CMOD*SUM)
50        CONTINUE
        AMOD1=PS*AMODT
        LMIN=1
        GO TO 70
60      LMIN=L2
70      CONTINUE
          DO 120 L=LMIN,L1
          L4=L+2*N
          IF(L4.GT.20)L4=25
          AMODT=0.D0
          IT=(-1)**(L+1)
            DO 100 M=LMIN,L4
            DELTA=IABS(L-M)
C
C       TEST TO SEE IF ASYMPTOTIC COULOMB WAVES ARE NECESSARY
C
            IF(R.GT.(RMAX/D))GO TO 80
            CALL COULC(R,L,DELTA,SUM,CMOD)
            GO TO 85
80          CALL COULCA(R,L,DELTA,SUM,CMOD)
85          DO 100 II=2,N2,2
            I=II-2
            IF(P(L+1,M+1,I+1).EQ.0.D0)GO TO 100
            AMODT=AMODT+F(N,I+1)*P(L+1,M+1,I+1)*DREAL(CMOD*SUM)
100         CONTINUE
C
C         PARTIAL WAVE SUM; AMOD1 = EVEN L WAVES
C                           AMOD2 = ODD  L WAVES
C
          IF(IT)104,120,106
104       AMOD1=AMOD1+AMODT
          GO TO 120
106       AMOD2=AMOD2+AMODT
120       CONTINUE
        INTGN=INTGN+(PS*AMOD1+PT*AMOD2)*(R**N2)*(EPSILN**N)/
       #DFLOAT(NFACT)
130     CONTINUE
        INTGN=INTGN/DEXP(0.5D0*(R/E)**2)
        RETURN
        END
C
C
C       SUBROUTINE COULA IS THE ASYMPTOTIC FORM OF COULO.
C       IT CALCULATES COULOMB WAVE FUNCTIONS IN THE FORM;
C
C       (2L+1)(I**L)EXP(I*DELTA(L)(SIN(KR+...)/KR
C
C
```

```
      SUBROUTINE COULA(R,L,SUM,MOD)
      IMPLICIT REAL*8 (A-H,O-Y)
      REAL*8 MOD,PI/3.14159265359D0/
      COMPLEX*16 SUM
      COMMON /AREA/ A,D,E,L1,L2,NMAX
      F=D*R
      ARG1=-0.5772156649D0
      ARG2=0.D0
      DO 20 J=1,50
      IF(J.LE.L)ARG1=ARG1+1.D0/DFLOAT(J)
      ARG2=ARG2+A/DFLOAT(L+J)-DATAN(A/DFLOAT(L+J))
20    CONTINUE
      ARG=A*ARG1+ARG2
      MOD=DFLOAT(2*L+1)*DSIN(F-A*DLOG(2.D0*F)-DFLOAT(L)*PI/2.D0
     #+ARG)/F
      SUM=DCMPLX(DCOS(ARG+DFLOAT(L)*PI/2.D0),DSIN(ARG+DFLOAT(L)*
     *PI/2.D0))
      RETURN
      END
C
C
C     SUBROUTINE COULCA IS THE ASYMPTOTIC FORM OF COULC.
C     IT CALCULATES THE PRODUCT OF COULOMB PARTIAL WAVES
C     DIFFERING BY "DELTA" UNITS.
C
C
      SUBROUTINE COULCA(R,L,DELTA,SUM,CMOD)
      IMPLICIT REAL*8 (A-H,O-Y)
      INTEGER DELTA
      REAL*8 MOD,PI/3.14159265359D0/
      COMPLEX*16 CMOD,SUM,PHASE
      COMMON /AREA/ A,D,E,L1,L2,NMAX
      F=D*R
      PHASE=DCMPLX(1.D0,0.D0)
      ARG1=-0.5772156649D0
      ARG3=0.D0
        DO 20 J=1,50
        IF(J.LE.L)ARG1=ARG1+1.D0/DFLOAT(J)
        ARG3=ARG3+A/DFLOAT(L+J)-DATAN(A/DFLOAT(L+J))
        IF(J.LE.DELTA)PHASE=PHASE*DCMPLX(DFLOAT(L+J),A)
20      CONTINUE
      ARG=A*ARG1+ARG3
C
      IF(DELTA.EQ.0) GO TO 30
C
      ARG2=DATAN(DIMAG(PHASE)/DREAL(PHASE))
      MOD=DFLOAT((2*L+1)*(2*(L+DELTA)+1))*
     #DSIN(F-A*DLOG(2.D0*F)-DFLOAT(L)*PI/2.D0+ARG)*
     #DSIN(F-A*DLOG(2.D0*F)-DFLOAT(L+DELTA)*PI/2.D0+ARG+ARG2)
     #/(F*F)
      CMOD=DCMPLX(MOD,0.D0)
      SUM=DCMPLX(DCOS(ARG2+DFLOAT(DELTA)*PI/2.D0),
     #DSIN(ARG2+DFLOAT(DELTA)*PI/2.D0))
```

```
      RETURN
C
C     DELTA=0 RETURN
C
30    MOD=(DFLOAT(2*L+1)*DSIN(F-A*DLOG(2.D0*F)
     #-DFLOAT(L)*PI/2.D0+ARG)/F)**2
      CMOD=DCMPLX(MOD,0.D0)
      SUM=DCMPLX(1.D0,0.D0)
      RETURN
      END
```

References

[1] Bromley, D.A.; Kuehner, J.A.; Almqvist, E.: Phys. Rev. Lett. 4, 365 (1960)

[2] Hanbury-Brown, R; Twiss, R.Q.: Nature 177, 27 (1956)

[3] Hanbury-Brown, R; Twiss, R.Q.: Nature 178, 1046 (1956)

[4] Cocconi, G.: Phys. Lett. 49B, 459 (1974)

[5] Beavis, D.; Fung, S.Y.; Gorn, W.; Huie, A.; Keane, D.; Lu, J.J.; Poe, R.T.; Shen, B.C. VanDalen, G.: Phys. Rev. C27, 910 (1983)

[6] Beavis, D.; Chu, S.Y.; Fung, S.Y.; Gorn, W.; Keane, D.; Poe, R.T.; VanDalen, G.; Vient, M.: Phys. Rev. C28, 2561 (1983)

[7] Zajc, W.A.; Bisterlich, J.A.; Bossingham, R.R.; Bowman, H.R.; Clawson, C.W.; Crowe, K.M.; Frankel, K.A.; Ingersoll, J.G.; Kurck, J.M.; Martoff, C.J.; Murphy, D.L.; Rasmussen, J.O.; Sullivan, J.P.; Yoo, E.; Hashimoto, O.; Koike, M.; McDonald, W.J.; Miller, J.P.; Truöl, P.: Lawrence Berkeley Laboratory Report No. LBL 17171, (1983)

[8] Zajc, W.A.; Bisterlich, J.A.; Bossingham, R.R.; Bowman, H.R.; Clawson, C.W.; Crowe, K.M.;Frankel, K.A.; Ingersoll, J.G.; Kurck, J.M.; Martoff, C.J.; Murphy, D.L.; Rasmussen, J.O.; Sullivan, J.P.; Yoo, E.; Hashimoto, O.; Koike, M.; McDonald, W.J.; Miller, J.P.; Truöl, P.: Phys. Rev. C29, 2173 (1984)

[9] Zarbakhsh, F.; Sagle, A.L.; Brochard, F.; Mulera, T.A.; Perez-Mendez, V.; Talaga, R.; Tanihata, I.; Carroll, J.B.; Ganezer, K.S.; Igo, G.; Oostens, J.; Woodard, D.; Sutter, R.; Phys. Rev. Lett. 46,1268 (1981)

[10] Lynch, W.G.; Chitwood, C.B.; Tsang, M.B.; Fields, D.J.; Klesch, D.R.; Gelbke, C.K.; Panagiotou, A.D.; Young, G.R.; Awes, T.C.; Ferguson, R.L.; Obenshain, R.E.; Plasil, F.; Robinson, R.L.: Phys. Rev. Lett. 51, 1850 (1983)

[11] Chitwood, C.B.; Aichelin, J.; Boal, D.H.; Bertsch, G.; Fields, D.J.; Gelbke, C.K.; Lynch, W.G.; Tsang, M.B.; Shillcock, J.C.; Awes, T.C.; Ferguson, R.L.; Obenshain, F.E.; Plasil, F.; Robinson, R.L.; Young, G.R.: Submitted to Phys. Rev. Lett.

[12] Bass, R.: Nuclear Reactions with Heavy Ions : Springer-Verlag, Berlin (1980) p. 215

[13] Koonin, S.E.: Phys. Lett. 70B , 43 (1977)

[14] Tanihata, I.; Nagamiya, S.; Schnetzer, S.; Steiner, H.: Phys. Lett. 100B ,121 (1981)

[15] Chrien, R.E.; Krieger, T.J.; Sutter, R.J.; May, M.; Palevsky, H.; Stearns, R.L.; Kozlowski, T.; Bauer, T.; Phys. Rev. C21, 1014 (1980)

[16] Boal, D.H.; Energetic Particle Emission in Nuclear Reactions: M.S.U. Preprint (1984) p. 16

[17] Westfall, G.D.; Gosset, J.; Johansen, P.J.; Poskanzer, A.M.; Meyer, W.G.; Gutbrod, H.H.; Sandoval, A.; Stock, R.: Phys. Rev. Lett. 37,1202 (1976)

[18] Gosset, J.; Gutbrod, H.H.; Meyer, W.G.; Poskanzer, A.M.; Sandoval, A.; Stock, R.; Westfall, G.D.: Phys. Rev. C16, 629 (1977)

[19]Von Weizsäcker, C.F.: Z. Physik, 96, 431 (1935)

[20] Stock, R.; Gutbrod, H.H.; Meyer, W.G.; Poskanzer, A.M.; Sandoval, A.; Gosset, J.; King, C.H.; King, G.; Lucker, C.; Nguyen Van Sen; Westfall, G.D.; Wolf, K.L.: Phys. Rev. Lett. 44, 1243 (1980)

[21] Stöcker, H.; Maruhn, J.A.; Greiner, W.: Phys. Rev. Lett. 44,

725 (1980)

[22] Stöcker, H.; Riedel, C.; Yariv, Y.; Csernai, L.P.; Buchwald, G.; Graebner, G.; Maruhn, J.A.; Greiner, W.; Frankel, K.; Gyulassy, M.; Schürmann, B.; Westfall, G.; Stevenson, J. D.; Nix, J.R.; Strottman, D.: Phys. Rev. Lett. 47, 1807 (1981)

[23] Chitwood, C.B. et al.: Private Communication

[24] Hale, G.M.; Dodder, B.C.: "Few-Body Problems in Physics". Elsevier, Amsterdam, Vol II (1984) p. 433.

[25] Chwieroth, F.S.; Tang, Y.C.; Thompson, D.R.: Nucl. Phys. A189,1 (1972)

[26] The data are taken from Figure 2 in Reference 10 for the reaction ^{197}Au(^{16}O,pp)X at a beam energy of 400 MeV.

[27] The figures are taken from Ref. 16 with permission.